The make-up of stars

Martin Asplund

Research School of Astronomy and Astrophysics, Australian National University, Cotter Road, Weston, ACT 2611, Australia

Abstract. The chemical composition of stars contain vital clues not only about the stars themselves but also about the conditions prevailing before their births. As such, stellar spectroscopy plays a key role in contemporary astrophysics and cosmology by probing cosmic, galactic, stellar and planetary evolution. In this review I will describe the theoretical foundations of quantitative stellar spectroscopy: stellar atmosphere models and spectral line formation. I will focus mainly on more recent advances in the field, in particular the advent of realistic time-dependent, 3D, (magneto-)hydrodynamical simulations of stellar surface convection and atmospheres and non-LTE radiative transfer relevant for stars like the Sun. I will also discuss some particular applications of this type of modelling which have resulted in some exciting break-throughs in our understanding and with wider implications: the solar chemical composition, the chemical signatures of planet formation imprinted in stellar abundances, the cosmological Li problem(s) and where the first stars may be residing today.

INTRODUCTION

The chronicle of the cosmos is written in starlight. Not only does the radiation from stars contain vital information about the stars and their histories, it also reveals the prevailing conditions before their births. Stars born at different times and locations can thus tell the whole story of the Universe from the earliest epochs a few hundred million years after the Big Bang when the first stars formed to the present day, from far-away galaxies to our solar neighbourhood. Indeed stars can even probe the conditions immediately after the Big Bang [e.g. 1, 2, 3]. Unfortunately it is not possible to extract the stellar properties directly from observations of their spectra. To decipher the information encoded in the starlight requires having realistic models for the formation of radiation at the stellar surface – the stellar atmosphere – as well as models how stars evolve with time. Of particular importance in this regard are late-type stars, which are the focus of this review: stars with masses not too dissimilar to the Sun. They are the most common stars on the night-sky and live for billions of years, making them extremely useful living fossils from bygone eras [e.g. 4, 5].

When Joseph von Fraunhofer first invented the spectroscope exactly two hundred years ago and discovered absorption lines in the solar spectrum the field of astronomical spectroscopy was born, which has remained an integral part of contemporary astrophysics and cosmology ever since. These Fraunhofer lines were subsequently explained by Kirchhoff in 1859 to originate from atomic transitions, paving the way for quantitative solar and stellar spectroscopy and the possibility to infer the elemental abundances of the Sun and other stars. Indeed the chemical compositions of stars enable astronomers to probe both cosmic, galactic, stellar and planetary evolution.

By necessity this review can impossibly cover all aspects of solar and stellar spectroscopy. I will unashamedly restrict the following discussion to late-type stars, both because of their importance for astronomy and because it is the field I know best. Furthermore, I will limit myself to describing in some detail only a few selected topics, again all dear to my own heart. I will first give a general overview of the art of modelling stellar atmospheres and spectroscopy (Sect.), including a discussion of the importance of convection for shaping the surface layers of late-type stars like the Sun and their spectra. The focus will be on more recent exciting developments in the field such as the emergence of 3D (magneto-)hydrodynamical models of stellar surface convection and atmospheres (Sect.) and detailed 3D and non-equilibrium spectral line formation (Sect.). These are topics that I'm convinced will transform the field in the coming decade and put the astronomical inferences related to for example stellar parameters and abundances on a much firmer footing.

The remaining part of the review will describe three particular applications of solar and stellar spectroscopy. I will first discuss the recent revision of the solar chemical composition – a fundamental yardstick in astronomy – which have partly been driven by advances in the modelling techniques (Sect.). While the new spectroscopically determined solar abundances in general have been warmly welcomed by most areas of astronomy, they do wreak havoc with the
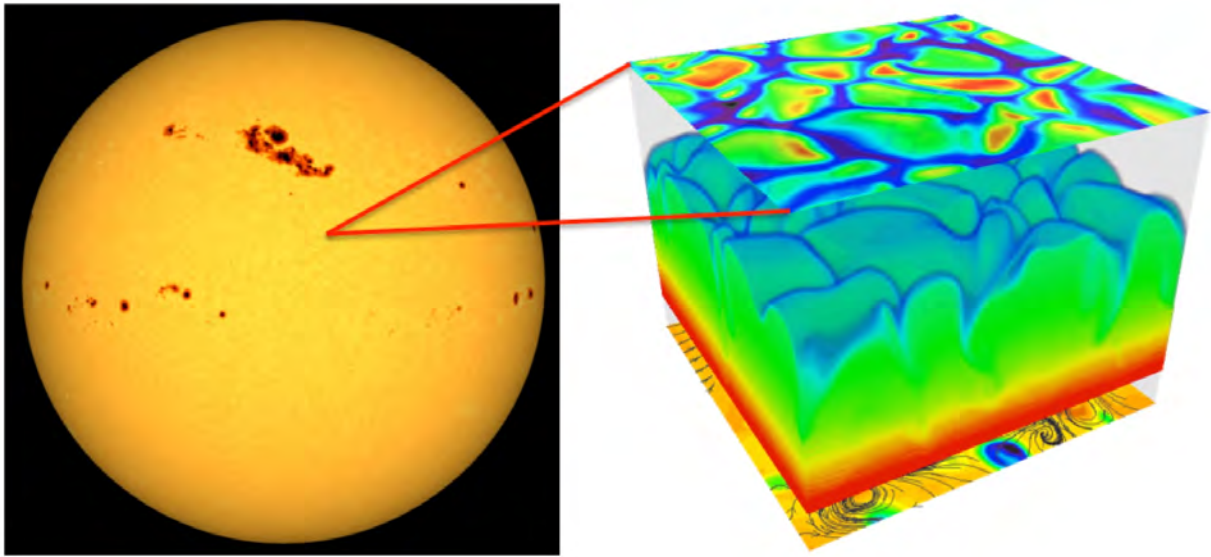
FIGURE 1. 3D (magneto-)hydrodynamical models of stellar surface convection and atmospheres solve the standard hydrodynamical equations of conservation of mass, momentum and energy coupled with the equation of radiative transfer in a small representative volume on the stellar surface, covering typically some ten granules (upflows) at any given time. The evolution of the convective motions and the atmospheric structure is followed in time over a few typical convective turn-over times. Such 3D stellar atmosphere models are used both to learn about the still poorly understood convection and magnetic fields under different stellar regimes and to interpret observed stellar spectra and oscillations.

solar interior, causing a major and still unresolved discrepancy with helioseismology (Sect.). The next part of the review will deal with whether the formation of planets imprints detectable signatures in the chemical compositions of stars (Sect.), which could shed light on the still poorly understood physical processes involved in planet formation and indeed on the origin of our own solar system. The last chapter of this review deals with the first generations of stars born after the Big Bang, some of which have survived to the present-day in our Galactic neighbourhood, relics of ancient times (Sect.). In particular I will describe how spectroscopy of such stars have revealed the presence of one or perhaps even two cosmological lithium problems, giving key insight to the physical conditions shortly after the Big Bang (Sect.). These stars are however extremely rare with many dedicated past, present and planned surveys to discover more of them with the hope that one day we may find a true first star born from pure primordial matter (Sect.).

TOOLS OF THE TRADE: STELLAR ATMOSPHERES AND SPECTROSCOPY

Stellar atmospheres: 3D stellar surface convection simulations

Fundamentally, classical stellar atmosphere models for late-type stars have not changed over the past half-century [e.g. 6, 7, 8]. While they have certainly improved in terms of input physical data (e.g. opacities) and completeness, the underlying assumptions still remain the same: gas in hydrostatic and thermodynamic equilibrium that does not change with time in a 1-dimensional (1D) geometry. Magnetic fields are ignored. Furthermore, the important convective energy transport is described through the rudimentary mixing length theory [9], which approximates convection with buoyant bubbles that rise a given distance (the so-called mixing length) before immediately dissolving and releasing its surplus energy. Solar granulation – the observational manifestation of the solar convection zone at the surface – directly testifies that this is a poor description of the physics of convection, which is very much 3D, dynamic and varying in time where magnetic fields play an important role [e.g. 10]. Rather than bubbles, solar convection is characterised by broad upflows and descending, finger-like plumes. Essentially all stars have one or more convection zones, indeed in most cases it reaches the surface layers and thus directly affects the emergent starlight in a similar manner as in the
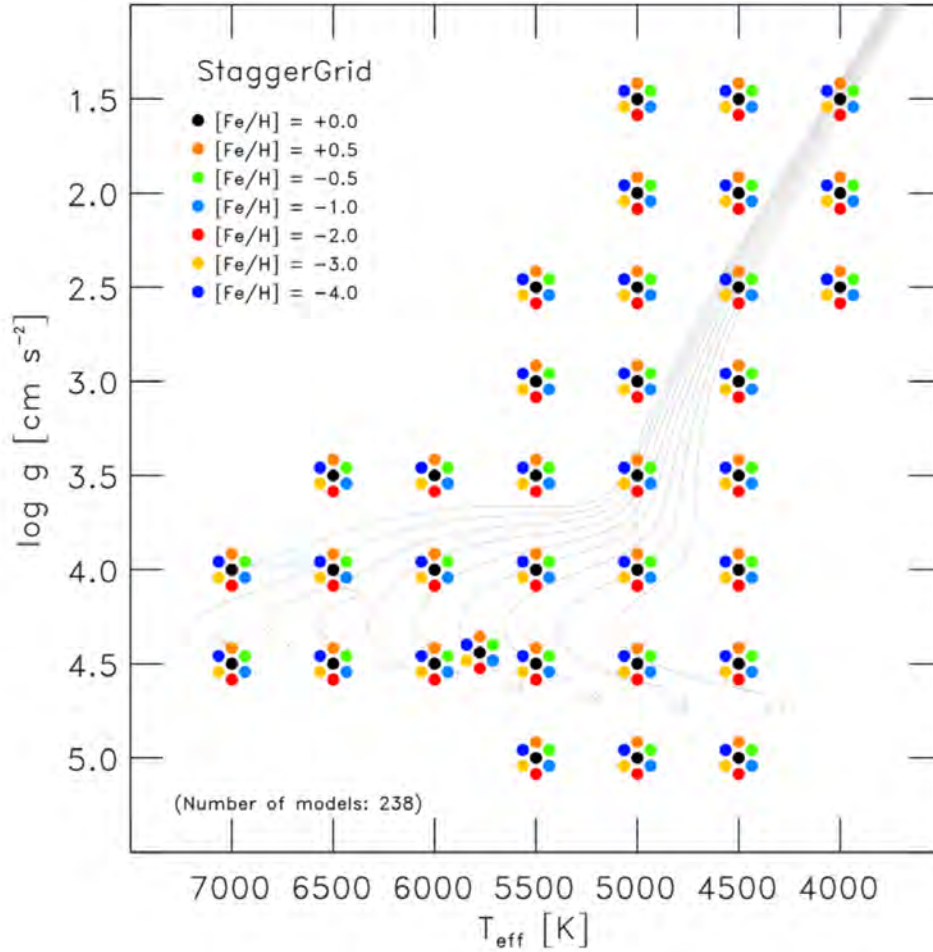
FIGURE 2. The coverage in the HR-diagram of the recently developed Stagger-grid [11] of 3D hydrodynamical models of stellar atmospheres, including a wide range of metallicities.

Sun [e.g. 11].

It is now possible to greatly improve stellar modelling by computing time-dependent, 3D, magneto-hydrodynamical simulations of stellar surface convection and atmospheres for a wide range of stellar parameters [e.g. 12, 13, 14, 13, 15, 16, 17, 11, 18]. Such 3D stellar atmosphere models solve the standard equations of hydrodynamics – conservation of mass, momentum and energy – together with a simultaneous solution of the radiative transfer equation in 3D for each time-step. Fully realistic equation-of-state and continuous and line opacities are used. The whole atmosphere of the star is not modelled but rather only a small representative volume of the surface from which the statistical properties over the whole star can be inferred (Fig. 1). The time evolution is followed on hydro-dynamical time-scales dictated by the requirement to cover at least a few convective turn-over time-scales of the simulation box to remove any effects of the initial stratification so that the 3D model has time to relax to the correct structures, i.e. hours in the case of the Sun. In order to make the 3D models computationally tractable, major approximations must be done for the solution of the 3D radiative transfer: local thermodynamic equilibrium is assumed and the opacity variations with wavelengths are incorporated by considering wavelength points with similar opacity behaviour together in a small number (typically 5-20) so-called opacity bins, a group-mean opacity approach [19]. Even under these severe approximations, the radiative transfer takes typically more than half of the total computing time.

Numerical 3D hydrodynamical simulations have fundamentally changed our view of how convection operates in stars [e.g. 20, 10, 11]: in contrast to the traditional view of buoyant bubbles raising from below as in the mixing length theory, the convection zone is driven by radiative cooling of the ascending gas at the surface. There is no unique mixing
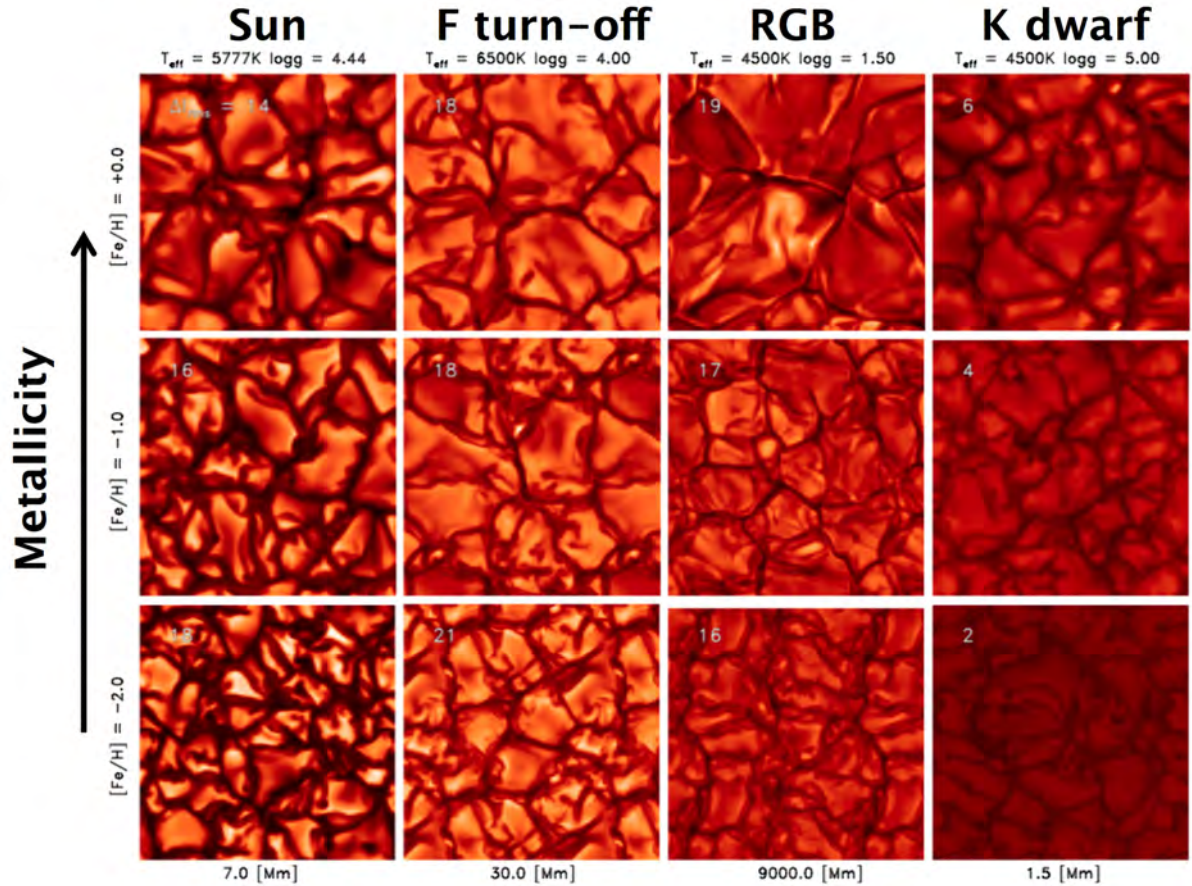
FIGURE 3. The appearance of granulation, the observable manifestation of convection, in different types of stars: the Sun, F-type turn-off star, RGB star and K dwarf, all for three different metallicities. While the physical dimensions differ wildly, overall the granulation pattern looks qualitatively the same with discrete warm, bright upflows (granules) and interconnected cool, dark downflows (intergranular lanes). The number in each panel gives the intensity brightness contrast in percent, showing that the granulation pattern becomes more pronounced at higher surface temperatures and lower gravities due to the larger convective velocities to transport the energy.

length: gas is overturning throughout the convection zone. Radiative transfer plays a critical role, while it is not even included in the mixing length theory. In fact the entire convection zone is driven by the radiative cooling in a very thin surface layer, which causes entropy-deficient gas to be accelerated downwards in finger-like down-drafts amidst gentle, broad upflows due to mass conservation (Fig. 4). This in turn results in (anti-)correlations between temperature, density and velocity of the typical granulation pattern. In the Sun, the typical convective velocities at the surface are a few km/s, slightly sub-sonic although shocks do appear prominently, especially where horizontal flows converge near where downdrafts are initiated.

While initially used to study solar granulation, these 3D surface convection simulations have been performed for different types of stars to investigate how convection operates in different stellar parameter regimes, from A stars down to brown dwarfs both for dwarfs and giants [e.g. 21, 17, 11, 18]. Here I'd like to highlight the work we have done with the Stagger code [22], the so-called Stagger-grid project. We have performed more than 200 high-resolution 3D hydrodynamical stellar atmosphere models, each with 12 opacity bins, covering $T_{\rm eff} = [4500, 7000]$ K, $\log g = [1.5, 5.0]$ [cgs] and $[{\rm Fe/H}] = [-4, +0.5]$, i.e. the regime of late-type stars in the HR-diagram (Fig. 2). We are using these 3D stellar models for a wide variety of applications besides learning about the nature of stellar convection and its dependence of stellar parameters, from stellar spectroscopy and abundance analysis [e.g. 23, 5] to improving stellar evolution modelling [e.g. 24] and helio-/asteroseismology (e.g. Muir et al., in prep.). The characteristic granulation pattern seen on the Sun is present for all late-type stars even if the exact appearance differs with stellar parameters
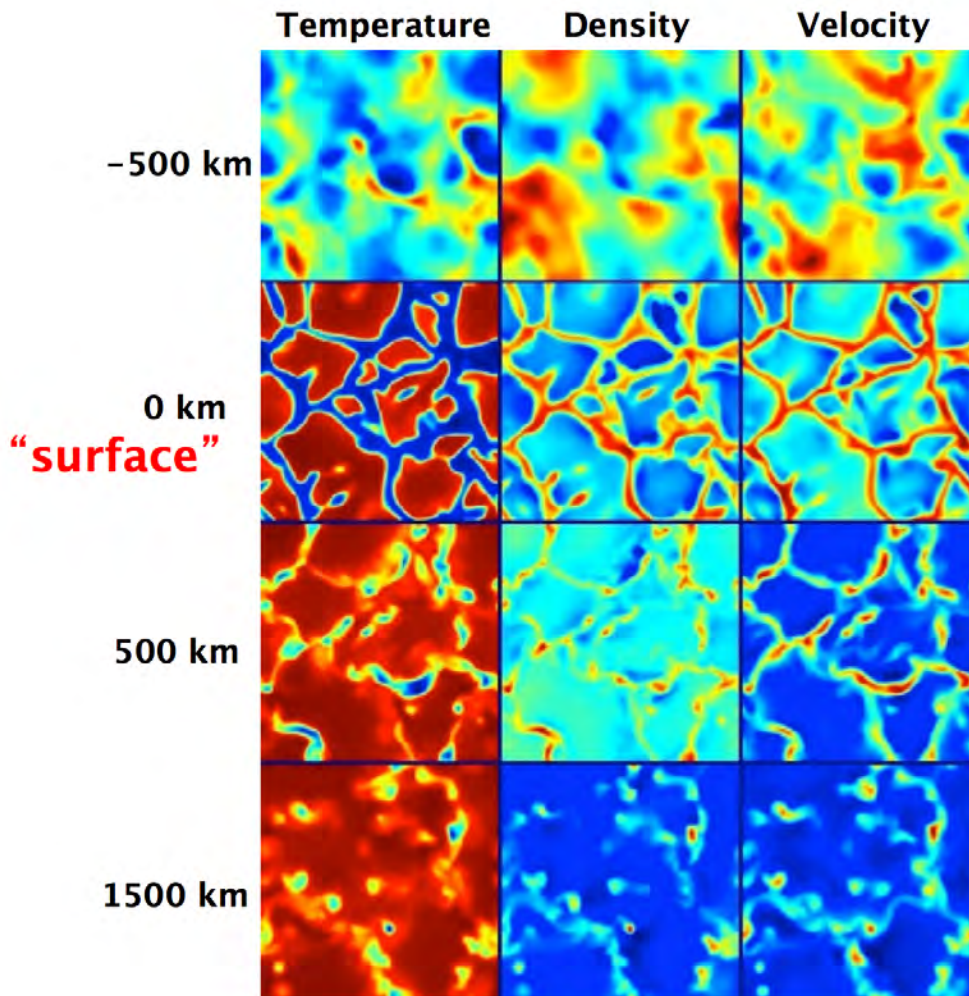
FIGURE 4. Horizontal slices of the temperature, density and velocity in a 3D hydrodynamical solar surface convection simulation at different depths; 0 km corresponds roughly to the visible surface seen in optical light. At the surface the temperatures and velocities are anti-correlated: warm gas is ascending while cool, dense gas is descending. The interconnected structure of downflows changes character below the surface to become finger-like downdrafts in the midst of broad, gentle upflows. Above the visible surface, energy transport is by radiation rather than convection and thus the (anti-)correlations between the variables are largely lost with the presence of waves and shocks. This is also the region where magnetic fields become dominant in the solar case, even in areas of the quiet Sun; this particular simulation lacks magnetic fields.

(Fig. 3): the granulation pattern is most prominent with the largest intensity brightness contrast at higher temperature due to so-called "naked granulation" [12] but also by lower gravity and (less so) with lower metallicity except at low temperatures.

A great deal of work has been carried out in showing that our solar and stellar surface convections are remarkably successful in reproducing key observational diagnostics, demonstrating that the 3D temperature, pressure and velocity structures are highly realistic, both in terms of their mean values as well as their horizontal fluctuations and temporal variations [10, 25]. For example whether a solar model has the correct mean temperature stratification can be empirically tested with the continuum centre-to-limb variation (Fig. 5). The 3D prediction agrees remarkably well with observations while all theoretical 1D hydrostatic models fail. Indeed our 3D solar model outperforms even the [26] semi-empirical solar atmosphere model that was constructed solely to fit these types of observations. Other crucial diagnostics that the 3D stellar models have been successful in reproducing include overall granulation topology (e.g. velocities, temperatures, time-scales, length-scales), intensity brightness contrast, flux distribution, spectral line
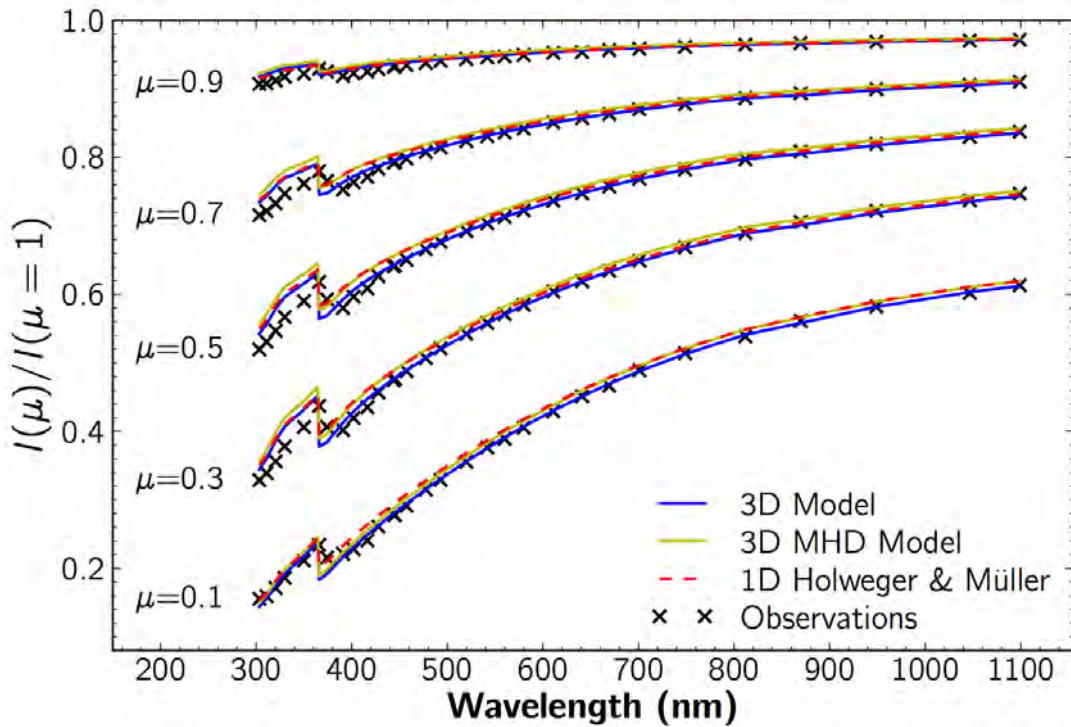
FIGURE 5. Observed (black crosses) and predicted continuum centre-to-limb variations for different solar model atmospheres: the 1D hydrostatic semi-empirical Holweger and Mueller [26], the 3D hydrodynamical model used by Asplund et al. [27] and a 3D MHD model [25]. It is noteworthy that the 3D models outperform even the Holweger and Mueller [26], which was constructed to fit the centre-to-limb variation. Somewhat surprisingly, the non-magnetic 3D model agrees better with observations than the 100 Gauss MHD model.

shapes, shifts and asymmetries both for spatially resolved and spatially averaged lines, H lines, centre-to-limb variation and solar oscillation frequencies [e.g. 10, 25]. Indeed the 3D solar model outperform all other tested 1D model atmospheres, be it theoretical or semi-empirical models, in every respect [25]. The fact that the 3D models pass the vast majority of the tests they have been exposed to with flying colours gives us confidence in applying such them to the interpretation of observed stellar spectra and oscillations.

Still the 3D hydrodynamical stellar atmosphere models are not perfect. The main challenge now is to include magnetic fields in the surface convection simulations as they are ubiquitous in stars. They manifest themselves in the solar atmosphere in a variety of ways, from small (< 100 km) bright pores to intense magnetic field concentrations in sun-/starspots and active regions covering a significant fraction of the surface [e.g. 28, 15, 29, 30]; similar phenomena are expected to be present in essentially all late-type stars [e.g. 31, , Magic et al., in preparation]. Whether a local or global dynamo operates in late-type stars to generate the magnetic fields is still not clear but convection must be a key ingredient. Likewise magnetic fields are likely responsible for heating of the solar corona and chromosphere, although exactly how is unknown.

Finally, it is possible to implement the crucial physics learnt from 3D convection simulations into stellar interior and evolution models, including using them as surface boundary conditions [13, 24, 32]. For example, it is possible to calibrate the mixing length theory by matching the entropy jump between the optical surface and the entropy of the upflowing material in the 3D surface convection models with the corresponding entropy structure of 1D interior models for the same stellar parameters (T_{eff}, $\log g$, [Fe/H]) computed with different mixing length parameters α_{MLT}. While the inferred mixing length parameter α_{MLT} is roughly constant along an evolutionary track from the main sequence to the red giant branch, there are systematic variations with mass [24, 32]. Unfortunately for the foreseeable future, full 3D stellar evolution modelling is beyond our computational abilities due to the wildly disparate dynamical and evolutionary time-scales bar special cases such as supernova explosions, making this chosen approach the perfect compromise.
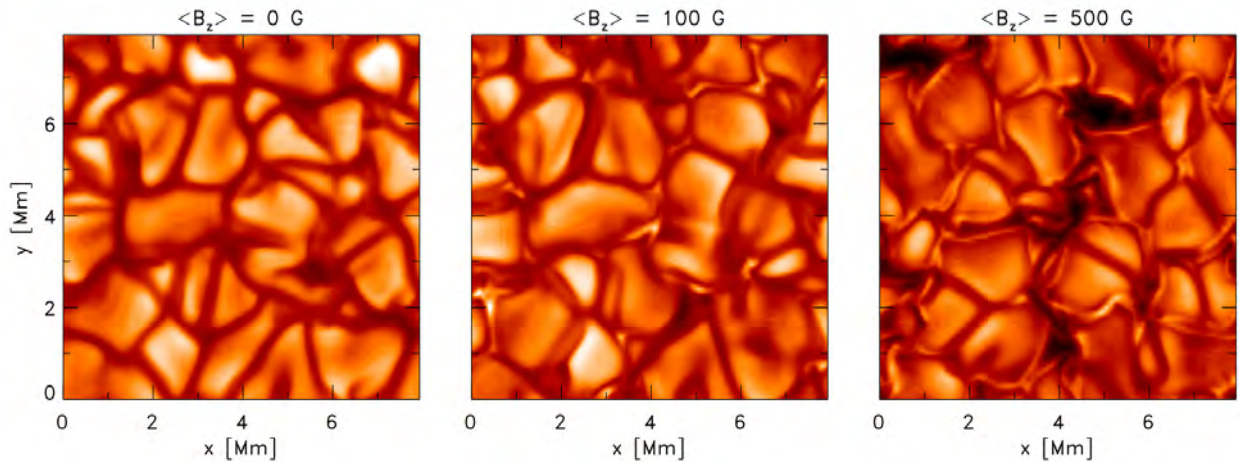
FIGURE 6. Appearance of solar granulation in 3D models with different magnetic field strengths: non-magnetic, 100 Gauss and 500 Gauss. The presence of magnetic fields gives rise to hot spots/lanes in the downflows, an optical depth effect allowing deeper and warmer layers to be seen, but also larger darker areas at large field strengths.

Stellar spectroscopy: 3D and non-LTE spectral line formation

Stellar spectra contain a wealth of information about the stars themselves and the environment in which they formed. To extract these data is however far from straightforward. Fig. 7 gives a schematic overview how one derives astrophysically relevant stellar properties, not-the-least their chemical compositions. An observed spectrum is compared with theoretical spectra computed by solving the radiative transfer equation in a given stellar atmosphere model corresponding to the various input parameters (effective temperature T_{eff}, surface gravity $\log g$, metallicity [Fe/H], chemical composition [X/Fe] etc) while relying on atomic physics data for each relevant transition (wavelengths, excitation potentials, transition probabilities, broadening parameters etc). The calculation of the synthetic spectrum is what could be considered the physics part of the problem while finding the combination that agrees best with the observed spectrum by changing the input parameters in an efficient and robust manner is a mathematics or numerical problem. Once the optimal solution has been identified can the astrophysical information be extracted.

In this Section I will not consider the fascinating topic of how to numerically find the optimal solution and instead focus on the physics part of the problem, especially how the radiative transfer is done. For late-type stars, traditionally theoretical stellar spectra are based on the restrictions of 1D hydrostatic stellar atmosphere models and line formation in local thermodynamic equilibrium (LTE), i.e. the atomic level populations are fully described by the Boltzmann and Saha distributions and the source function in the radiative transfer equation is equal to the Planck function. Nowadays the scene is slowly changing with the possibility of employing 3D hydrodynamical stellar models as described above. Similarly, non-LTE line formation calculations are feasible, provided the necessary atomic data for a huge number of transitions are available [33].

There a several advantages with using 3D stellar atmosphere models. Firstly, they should be more realistic than classical 1D models given their more sophisticated and physically more motivated foundation and indeed systematically perform better for all investigated observational tests [25]. Secondly, they render the use of the traditional fudge-factors in stellar spectroscopy – micro- and macroturbulence – obsolete. Instead the necessary line broadening is fully provided by the Doppler shifts introduced by the convective motions and oscillations in the atmospheres [34]. Thirdly, they are far more versatile than 1D models, being able to be used for different purposes.

One case where 1D models can not be used but 3D hydrodynamical model atmospheres can is spatially resolved spectroscopy. Line profiles vary radically across the stellar disk, depending whether it is an up- or downflow [e.g. 36, 34]: in the upflows the continuum intensity is high, the profiles are blue-shifted and the lines are typically strong as a result of the steep temperature structure while in the descending gas the continuum intensity is low and the lines are red-shifted and weak. How large these variations are depend on the details of the line formation, such as formation height and how tightly coupled the radiation field and gas are (in other words, whether LTE is a good approximation or not). Fig. 8 shows a few examples of lines with different properties in the solar case. Clearly, the observed variations are exceptionally well reproduced by predictions from the 3D hydrodynamical model [35], which increases the confidence
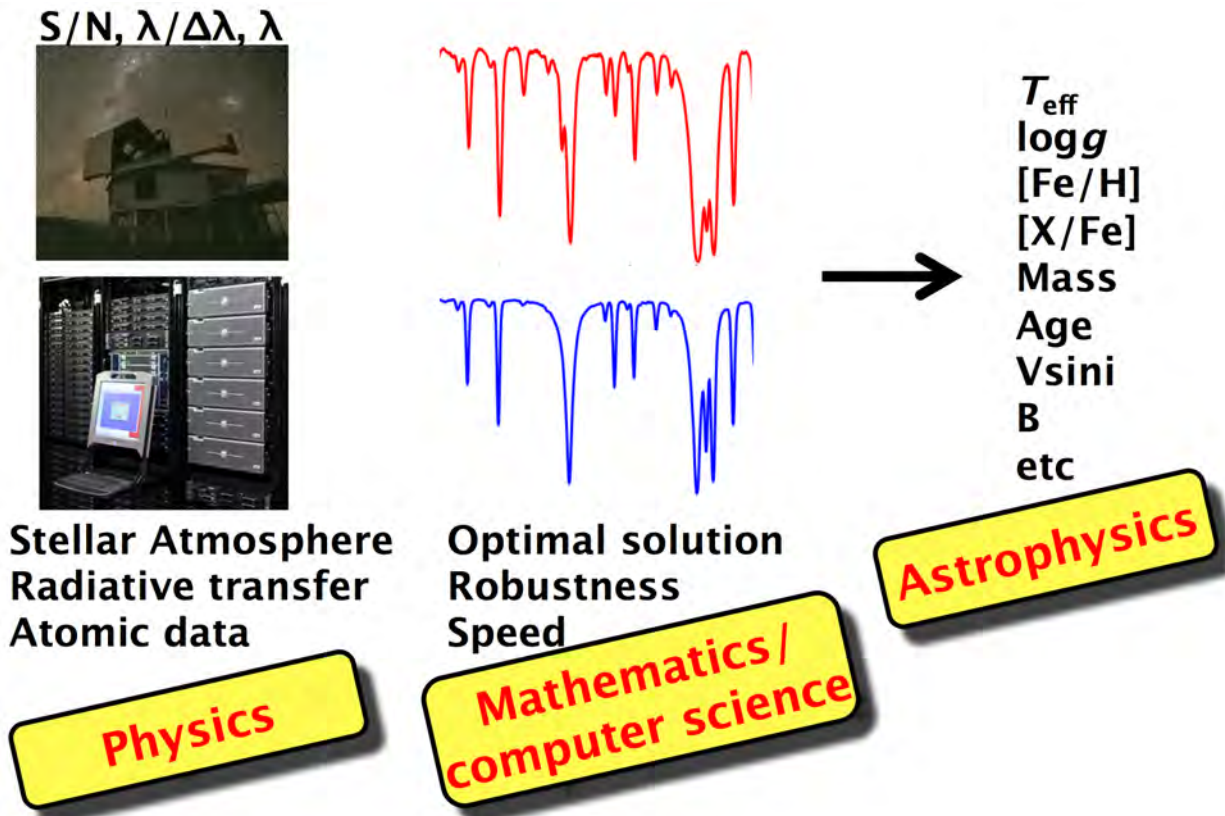
FIGURE 7. Schematic overview of how quantitative stellar spectroscopy is done. To derive astrophysical properties of stars require to compare an observed stellar spectrum with a theoretical spectrum computed by solving the radiative transfer through a model atmosphere of given stellar parameters with the results also heavily dependent on the accuracy of the atomic data. The stellar parameters are then modified to find the obtain solution that agrees best with observations.

further in the model being a highly realistic description of the solar photosphere.

In the case of the stars, we observe spatially and temporally averaged lines. Because of the correlations between continuum intensity, line strength and line shift, the resulting averaged line profile will be asymmetric with a characteristic C-shape bisector typically [e.g. 36, 34]. As such the detailed line shape is a very sensitive probe of the statistical properties of the atmospheric conditions and convective motions. Current 3D hydrodynamical models of solar and stellar atmospheres are remarkably successful in reproducing the exact profiles of spectral lines, including their shifts and asymmetries resulting from convection, which furthermore is achieved without any free parameters in the modelling [34]. Indeed the only property allowed to vary is the abundance of the element in question, lending strong support to the correctness to the inferred abundance.

In recent years, a large number of studies have been employing 3D radiative transfer under the assumption of LTE to derive solar and stellar abundances [e.g. 14, 37, 38, 16, 39, 40, 41]. While the 3D models should be more realistic than traditional 1D model atmospheres, care should still be exercised when interpreting the results as the simplification of LTE could be highly misleading. This is particularly true for metal-poor stars in which the 3D temperature structure is much cooler in the higher, optically thin layers than corresponding 1D models [14]: the steep temperature gradient gives rise to a hot radiation field from below that can drive significant departures from LTE for minority species and low-excitation lines [42]. For the Sun and similar stars, non-LTE effects tend to be relatively small, making 3D LTE calculations a reasonable approach, which however still need to be verified through non-LTE studies.

When relaxing the LTE assumption the complexity of the problem increases dramatically both conceptually and numerically. Rather than relying on the Boltzmann and Saha distributions for the atomic level populations, the rate equations for each level incorporating in principle every conceivable atomic transition must be solved simultaneously with the radiative transfer equation for every wavelength of relevance. In other words, the level populations depend
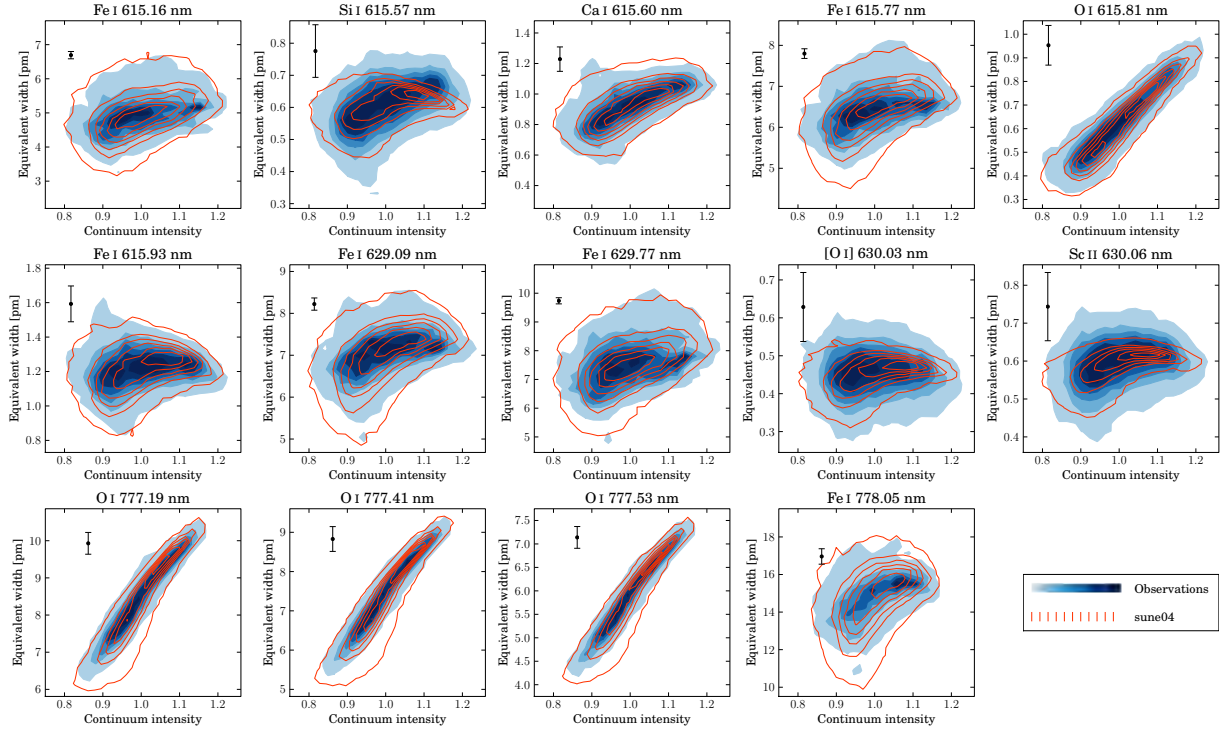
FIGURE 8. Spatially resolved lines in the Sun for a variety of lines with different properties in terms of excitation potential, line strength, formation height and sensitivity to non-LTE effects [35]. For line, the observed (blue contours) and predicted (red contours) equivalent widths across the granulation pattern is plotted as a function of the local continuum intensity. In the case of O I lines, full 3D non-LTE calculations have been carried out while for the rest the assumption of LTE is made. The excellent agreement for all lines is a very good testament to the realism of the employed 3D hydrodynamical solar model atmosphere.

on the mean intensity of the radiation field J_ν at all locations and frequencies due to the non-locality of the radiation field and the coupling through the different transitions: Everything depend on everything, everywhere else! Naturally this problem is normally simplified, first by assuming statistical equilibrium (i.e. the time-dependence is ignored) and second by only including the most relevant levels and transitions. Furthermore, for late-type stars, non-LTE invariably assume that the element under consideration is a trace element: departures from LTE do not feed back into a different atmospheric structure. Still the required model atom is often substantial with hundreds of levels and thousands of radiative transitions, each described with tens or hundreds of wavelength points. For each wavelength the radiative transfer equation must be solved to compute J_ν and thus the rate equations. To find a consistent solution for both J_ν and the level populations then requires to iterate in a clever fashion, requiring typically tens of iterations. A further challenge is to compile the necessary atomic data for these vast number of transitions. Often the data do not exist, especially for collisional cross-sections and therefore classical, order-of-magnitude (at best!) estimates have to be applied [e.g. 43, 44], rendering the results sometimes rather uncertain.

In 1D, non-LTE calculations are easily tractable numerically, with many recent studies devoted to different elements of astrophysical importance [e.g. 45, 46, 47, 48, 49, 50]. Going to 3D increases the computational demand dramatically however. To date only a few full 3D non-LTE calculations have been performed with the aim of deriving solar or stellar abundances, such as Li in the Sun [51, 52] and in metal-poor stars [42, 53, 3] and O in the Sun [54, 35]. No doubt this will be an active area of research in coming years given the great importance of deriving accurate elemental abundances and the ever-increasing computational power available. In the short-term an alternative and faster approach is to use the horizontally and temporally averaged 3D hydrodynamical models, $< 3D >$ models, as 1D equivalent models. This has numerous advantages: 1) standard 1D non-LTE codes can be used (very few 3D non-LTE codes are publicly available and they are often still under development or not yet fully stress-tested given the novelty of the field); 2) calculations are much faster; and 3) the main effect of the 3D models, the more realistic temperature structure, is still accounted for. Obviously the full details can never be captured in 1D and the fudge factors micro- and macroturbulence must still be retained. The first such $< 3D >$ non-LTE calculations are now starting to appear for selected elements [e.g.

55, 56, 57].

THE EFFECTS OF SUNLIGHT: DOES THE SUN HAVE A SUB-SOLAR METALLICITY?

Solar chemical composition inferred from spectroscopy

The solar chemical composition is a fundamental yardstick in astronomy to which essentially all measurements of the elemental abundances of planets, stars, galaxies and interstellar/intergalactic medium is referenced. Work on improving the accuracy in the solar abundance determinations is thus of major importance with implications for the rest of astronomy, as for example evident from the massive number of citations garnered by the careful compilations of the solar chemical composition: the seminal work of Anders and Grevesse [58] is the sixth most cited astronomy publication ever published with well over 6000 citations! Solar analyses are time-consuming, involving necessary improvements on a diverse front, including not-the-least the wonderful work of a relatively small number of atomic physicists devoted to these endeavours. As such a large number of groups have contributed over the years, focusing on their specific parts or elements of interest. Until recently, all tabulations of the recommended solar photospheric abundances were therefore compilations of the results from other publications, each with their own analysis techniques, ingredients and assessment of uncertainties [e.g. 58, 59, 60, 61, 62].

We have recently completed the first ever homogeneous analysis of the solar chemical composition in which all elements were treated in the same manner [27, 56, 57, 63]. Furthermore, our study was the first to systematically employ a realistic 3D hydrodynamical solar atmosphere model and 3D line formation calculations in an attempt to increase the accuracy and remove remaining systematic errors in the measurements. We spent considerable time scouring the atomic physics literature to locate the best possible input data such as transition probabilities and were highly selective in the employed lines, restricting the analysis to only the cleanest spectral lines with reliable atomic data. The use of suboptimal lines will always increase the scatter but also tend to skew the resulting abundances to too high values due to the presence of unaccounted for blends; it is best to err on the side of caution. Finally we attempted to quantify in great detail the remaining uncertainties, both statistical and systematic. The result is the most accurate determination of the solar chemical composition possible today with state-of-the-art analysis methods and a very careful consideration of the analysis ingredients and uncertainties, all done homogeneously for every element.

The main difference compared with previous solar abundance work of our new analysis is a rather dramatic downward revision of the solar abundances of C, N and O (which in turn also implies a similar adjustment of the solar Ne abundance that can not determined directly spectroscopically, [27]) by 30-40%. This may not sound like much in an astronomical context where errors of factors of several are common-place but remember again that this is a change to a yardstick in astronomy. Furthermore, C, N, O and Ne are the most abundant metals (elements heavier than He) in the Sun and the Universe, which are of major astronomical importance, including for galactic and stellar evolution as well as for planetary physics. Overall the bulk solar metal content decreases from 2% to 1.4% (Fig. 9); see Asplund et al. [27] for a discussion how the present-day photospheric abundances are converted to the initial bulk composition after accounting for gravitational settling over the course of the Sun's 4.5Gyr lifetime.

It is often said that the new solar abundances of Asplund et al. [27] are down to their use of a 3D model atmosphere. This is however only partly correct as there are other important factors as well. Take for example the case of oxygen. There are multiple indicators of the solar O abundance: low-excitation, forbidden [O I] lines, high-excitation, permitted O I lines, vibration-rotation lines of OH and pure rotation lines of OH, all with their own sensitivities to the atmospheric conditions and with high-quality atomic data and observations readily at hand. Previously, most studies found quite conflicting results from the different types of lines, making it difficult to select which abundances to trust the most as each have their pros and cons. Now it turns out that in each case different dominant factors are at play for pushing down the inferred solar abundance. For the [O I] lines the main cause is previously overlooked blends [e.g. 37, 54, 64, 35, 65, 66] while departures from LTE are prominent for O I [e.g. 54, 35]; in both cases quite similar results are obtained when using the semi-empirical Holweger and Mueller [26] solar model that has traditionally been used for solar abundance analyses. The ability of the 3D solar model to very accurately predict the detailed line shapes was however instrumental in realising that the [O I] lines are indeed significantly blended, especially the 630.0 nm line with a suspected but ignored Ni line [67, 68]. Only in the case of the OH lines is the main culprit the use of the 3D model. These lines are, as essentially all molecular lines in solar-type stars, very temperature sensitive and both the cooler mean stratification and the presence of temperature inhomogeneities in the 3D model lead to stronger OH lines and
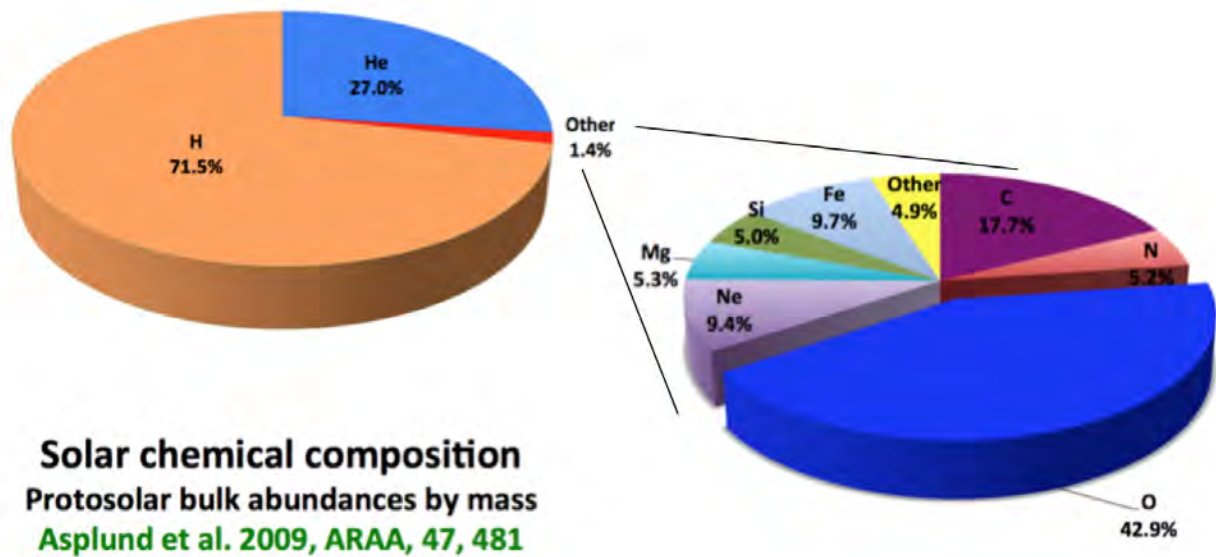
FIGURE 9. The proto-solar bulk elemental abundances by mass from Asplund et al. [27]. The elements heavier than He only constitute 1.4% of the mass in the Sun with O, C, Ne and N (in order of importance) being the most abundant.

thus a lower O abundance is required [e.g. 54]. Similar arguments hold for C and N where both atomic and molecular lines are available, something which is not possible for any other elements in the solar spectrum except for H.

Given the major change compared with the previous recommended solar abundances, it is reasonable to ask how reliable the new values really are. As already mentioned, the analysis of Asplund et al. [27] was carried out with utmost care using state-of-the-art tools and input data relying only on the best lines. Still not everything is fully settled as some other groups get somewhat differing results. Most of the attention has naturally focussed on O and to a lesser extent C and N; other elements are less in dispute in general. In particular Caffau et al. [40] have used their own 3D solar model computed with the CO5BOLD code [21] to derive the solar C, N and O abundances [65, 69, 70] and find in general intermediate values compared with Asplund et al. [27] and those recommended by Grevesse and Sauval [59]. The two 3D models are in fact very similar [17] with instead the differences boiling down to selection of lines, adopted atomic data, observational data and non-LTE corrections. It is perhaps telling that their abundance scatter is always substantially higher than ours, a clear indication that suboptimal lines have been employed due to for example blends or inaccurate atomic data; as mentioned above, this tends to skew the results upwards. They have not considered molecular lines nor have they exposed their analysis techniques to the same level of observational tests as we have done, for example centre-to-limb variations and spatially resolved solar spectroscopy [35, 25].

An almost unavoidable question after each talk on the new solar abundances is *"Yes, but what about magnetic fields?"* Fabbian et al. [71, 72] have performed 3D MHD solar granulation simulations for a range of magnetic field strengths and investigated the impact on spectral line formation. They found that the main effects on the solar photospheric structure for modest magnetic fields is a concentration of the field strength in downflows as expected with upflows being divergent flows (Fig. 6) and a slight increase in the mean temperature in optically thin layers ($\Delta T_{\rm eff} \approx +70\,{\rm K}$ at $\log \tau_{500} = -3$) due to increased magnetic dissipation. As a result, when restricting to magnetically insensitive lines, i.e. those with small Landau factor, the impact on the solar abundance analysis is small with the inferred abundance from typical Fe I lines increased by 0.01-0.04 dex depending on the line formation region (i.e. line strength and excitation potential). We have carried out an analogous study using our own 3D MHD simulations for different field strength and find that the impact on the lines employed for our solar abundance analysis is very small in general, typically $0.01 - 0.02\,{\rm dex}$, for the 100 G simulation (Asplund et al., in preparation). One exception is molecular lines which are formed in higher atmospheric layers and thus more sensitive to the higher temperatures in the MHD models. In the case of OH, the MHD-based O abundance is $\approx 0.05\,{\rm dex}$ higher than for the pure hydrodynamical model, which would shift the mean solar O abundance up by $\approx 0.03\,{\rm dex}$ relative to the derived value in Asplund et al. [27]. It should be noted however that the 100 G MHD solar model performs worse than the hydrodynamical model against an arsenal of observational diagnostics [25] and thus it is not obvious whether the MHD-results are indeed more trustworthy.
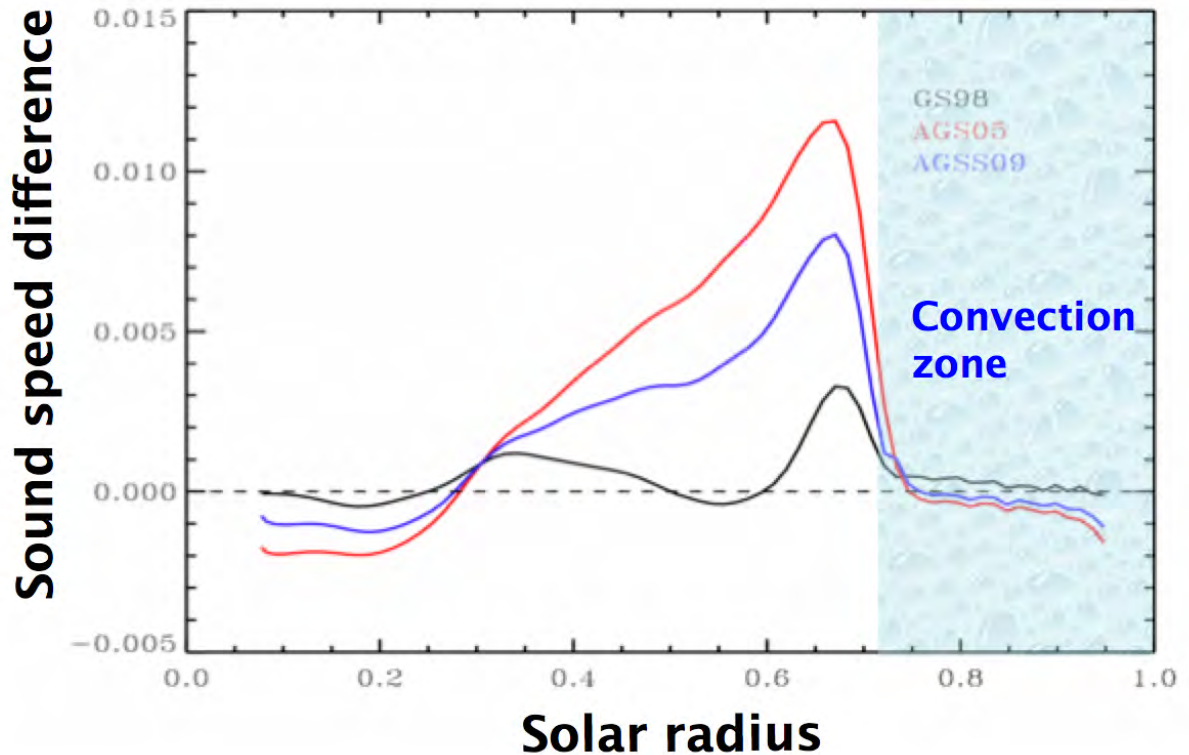
FIGURE 10. The difference between the predicted sound speed from solar interior models with the inferred sound speed from helioseismology [75]. Three cases are shown using the recommended solar photospheric abundances of Grevesse and Sauval [59] (black line), Asplund et al. [61] (red line) and Asplund et al. [27] (blue line). The largest discrepancy occur immediately below the convection zone which covers the outer ∼ 30% in the Sun (shaded region).

Clearly improving the 3D MHD models further for solar abundance analysis purposes is high on the agenda for the coming years.

Helioseismology and the solar modelling crisis

The new solar abundances presented by Asplund et al. [27] in general work better than the older values for a variety of astronomical circumstances but in one case they wreak havoc: solar interior models and helioseismology. Since C, N, O and Ne are important opacity sources in the interior, especially immediately below the convection zone, the new lower abundances change the interior stratification which then come into conflict with the helioseismic evidence [e.g. 73, 74, 75]. Not only is the sound speed in error (Fig. 10), but so is the predicted depth of the convection zone and the He abundance. It is noteworthy that older recommended solar abundances such as those by Grevesse and Sauval [59] agree much better with helioseismology.

This so called solar modelling crisis has been around for about a decade now since the first studies finding a low solar O abundance appeared [37, 54] and there are no signs that the problem is abating. A large number of proposed solutions have been put forward, some more plausible than others, yet none has stood the test of time [see e.g. discussion in 74]. One possibility is of course that our derived 3D-based solar abundances are to blame. At this stage I consider this unlikely, at least in a serious sense to overcome the discrepancy with helioseismology. We have carried out extensive testing of both the 3D solar model and the 3D line formation calculations and in all cases they perform extremely successfully [25]. Furthermore, the different C, N and O abundance indicators agree very well with each other in spite of having often completely different sensitivities to possible systematic errors. Finally, we infer similarly low abundances when instead employing the venerable Holweger and Mueller [26] semi-empirical model.

Another possibility is that standard solar interior and evolution modelling lack some important ingredient. This is not too far-fetched given that such models still rely on a 1D geometry and treat convection through the rudimentary mixing length theory. Indeed it may be telling that the largest discrepancy occurs immediately below the convection zone, which may be related to the fact that these solar models can not predict the substantial Li depletion that has occurred over the solar lifetime. Recent work on solar twins convincingly demonstrate that this Li depletion proceeds throughout the life of star like the Sun and is not restricted to the pre-main sequence evolution [76]. This additional mixing below the convection may be caused by internal gravity waves [77].

Perhaps the most obvious possibility is that the opacities used in stellar interior calculations are not quite right. To compensate for the lower C, N, O and Ne abundance would require an increase in the Rosseland opacities by $\sim 20\%$ below the convection zone [e.g. 75]. While a few years ago atomic physicists involved in such large-scale opacity calculations were very reluctant to admit to such a possibility, lately many of them have come around to this prospect. New calculations treating K-shell ionisations in more detail do indeed find substantially more resonances and thus higher overall opacities than in the original Opacity Project calculations [78]. Excitingly, similar conclusions are coming from novel experiments using for example Sandia's Z-Pinch national facility in the US where opacities can be measured for conditions directly corresponding to those existing below the convection zone in the Sun (Bailey et al., in preparation).

It is crucial to remember that whatever the solution to the solar modelling crisis turn out to be, this is not a *solar* physics problem but a *stellar* physics problem: any solution will impact how we study other stars. For example if missing opacities are the explanation, then all stellar evolution calculations will be affected at least to some degree, requiring whole new set of evolutionary models and isochrones. If on the other hand, the new solar photospheric abundances are not trust-worthy for whatever reason (which I hope is not the case), then it is back to the drawing board before we can tackle other stars spectroscopically with what are supposed to be the most sophisticated tools we have available: 3D hydrodynamical model atmospheres and non-LTE radiative transfer.

HEAVY METAL, ROCKS, STARS: CHEMISTRY OF PLANET-HOSTING STARS

Understanding how planets form and evolve, both in our own solar system and around other stars, is a central pillar in modern astronomy. Indeed the search for extrasolar planets and their characterization is a – if not the – main driver behind the next generation of multi-billion dollar astronomical facilities currently under construction or being planned. Today more than 1000 extrasolar planets are known, a remarkable feat given that the first exoplanet orbiting a solar-like stars was discovered not even two decades ago [79]. These planets have been discovered through a raft of ingenious methods, the most successful being radial velocity variations in the stellar spectrum due to the gravitational tug and corresponding Doppler shift from the (unseen) planet and variations in stellar brightness due to the planet transiting in front of the stellar disk. The most astonishing fact is perhaps not the great number in which planets are now known but the enormous diversity in their properties [e.g. 80]. The vast majority of the discovered extrasolar planets are gas giants like Jupiter but orbiting close to their host stars, quite unlike the solar system planets. This is partly an observational selection effect since such planets are easier to detect but it is clear that planets come in amazing assortment of types. As the observational techniques are refined and the time baseline increases, planets with smaller masses as well as on longer orbits will be discovered, although it will likely be another several years until a habitable Earth-sized planet orbiting a star like the Sun at a similar distance is detected, extraordinary satellite missions like Kepler [81] notwithstanding. The yield of Kepler planetary candidates clearly demonstrates, however, that statistically at least Earth-sized planets are surprisingly common [82].

Stars and their planets are thought to arise from the same fragment of a collapsed molecular cloud. Consequently, a star's properties likely reflect the physical conditions of the disk its planets formed in. Furthermore, coupling between stars and their proto-planetary (accretion) disks, perhaps through magnetic fields, suggests that the evolution of young planetary systems could affect the evolution of their host stars. Therefore, the study of correlations between properties of planets and the characteristics of their host stars can give crucial insight to planet formation, which is still very poorly understood. One of the key results that has emerged in the field of exoplanet science has come from investigations in the area of the star-planet connection. Soon after the first extrasolar planet was reported, a strong positive correlation between the metallicity of the host stars and the probability of finding planets was identified [e.g. 83, 84, 80]: at solar metallicity at least 4% of stars have giant planets, which increases to 30% at the highest metallicities; these are obviously lower limits due to observational limitations. This metallicity-dependence is typically interpreted as support for the core accretion model of giant planet formation [85] while in the rival disk instability model [86] no such correlation is necessarily expected. This dependence can naively be understood: with an increased metallicity, more
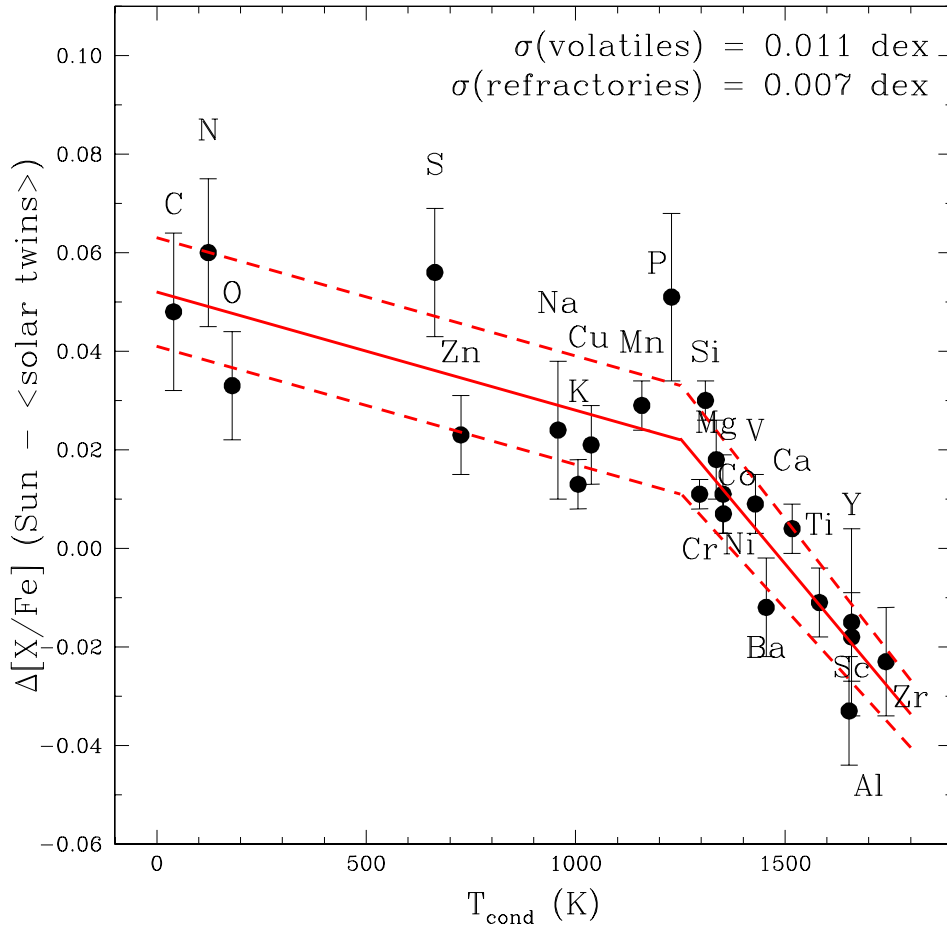
FIGURE 11. Differences in chemical composition between the Sun and the average of 11 solar twins as a function of dust condensation temperature as inferred from a line-by-line differential analysis using extremely high-quality MIKE/Magellan spectra [94]. The trend that refractory elements (high condensation temperature) are systematically more deficient in the Sun compared with the solar twins is highly statistically significant given the very high precision achieved. Meléndez et al. [94] interpreted this as a tell-tale chemical signature of planet formation: for whatever reason planet formation proceeded more efficiently around the Sun than for the typical solar twin.

elements that can condense into dust are available. The dust then grows through successive collisions to form rocky and icy planetesimals, which can either start runaway gas accretion to form giant planets or form rocky planets through successive collisions. The exact details how planet formation proceeds still pose enormous theoretical challenges in spite of recent progress [e.g. 87].

In addition to the effects of overall metallicity, individual elemental abundances of host stars are of great interest, since the exact composition may dictate what type of planets will form [88]. Some elements may have an outsized role in forming planets, such as Si for rocky planets or O for gas giants [89], which may be reflected in the stellar abundances. Likewise, planet formation may imprint detectable abundance signatures in the stars either by removing chemically fractionated material locked up in the planets from the gas accreted onto the proto-star or by the engulfment of whole planets by the star [90]. Some correlations have been suggested but those results are either disputed or disproven through more refined analyses. One example is the case of lithium, which has been claimed to be less abundant in stars with planets [91, 92] but it has subsequently been demonstrated that selection biases may invalidate their conclusions [93].

Many groups have searched for specific chemical fingerprints as a way to differentiate stars with and without

planets but with limited success. Recently however the telltale marks of planet formation in the observed solar and stellar chemical compositions have been identified. Through one of the most precise stellar abundance analysis ever accomplished, Meléndez et al. [94] have demonstrated that the Sun has a peculiar abundance pattern compared with typical solar-like stars (Fig. 11); these results have subsequently been confirmed by Ramírez et al. [95, 96]. The Sun is not unique but unusual: only $\sim 15\%$ of stars share the Sun's detailed chemical composition. The abundance differences correlate strongly with the condensation temperatures of the elements: refractory elements that easily form dust like Fe and Mg are deficient in the Sun relative to the volatile elements like C and O. While Fig. Fig. 11 would seem to suggest that the Sun is slightly enhanced in the volatile elements, this is a result of Fe having been chosen as the reference element ($T_{cond} = 1334$ K); had instead say C been chosen as the reference, all stars, including the Sun, would share the same abundances of the volatiles while the refractories would be correspondingly more depleted. The relative abundance differences are very small (< 0.08 dex, i.e. $< 20\%$), which explains why previous studies have not succeeded in detecting the correlation due to lack of the necessary accuracy. Doing a strictly differential line-by-line analysis of stars essentially identical to each other with exquisite quality spectra obtained from the same instrument is crucial to achieve such a high precision: the typical uncertainties and systematic errors (e.g. atomic data, stellar parameters, non-LTE, 3D effects) then largely disappear, making it possible to reach the sub-0.01 dex level in abundance precision [97].

What is the origin of the peculiar solar abundances? Stellar nucleosynthesis can be ruled out as an explanation for this pattern as it would have different elemental signatures. Instead the correlation with condensation temperature implies a connection with planet formation, because dust condensation is a necessary first step in the process of forming planets via core accretion. The scenario Meléndez et al. [94] envisioned sees the refractory elements being preferentially locked up in planetesimals (and subsequently planets) compared with the more volatile elements while the remaining dust-cleansed gas continue to be accreted onto the Sun [94]. For whatever reason planet formation proceeded more efficiently in the solar system than for typical stars.

There are even tantalizing hints that these chemical fingerprints stem from the formation of the terrestrial planets rather than the gas giants, which, if confirmed, would be a remarkable finding with great potential to learn more about planet formation. Firstly, the amount of material required to produce this abundance signature (assuming the dust-depleted accretion took place once the solar convection zone reached roughly its present-day size) amounts to about 4 Earth-masses, which is surprisingly similar to the 1.3 Earth-masses available in the terrestrial planets [94, 98]. Secondly, and perhaps more telling, the break at $T_{cond} \approx 1200$ K in Fig. 11 suggests that most of the dust condensation happened close to the proto-Sun and not where the gas giants formed. Thirdly, if a star has been confirmed not to have a close-in giant planet, the probability for it to share the solar composition is $\sim 70\%$ rather than the typical $\sim 15\%$ for all stars when no planet information is available [94]. In any case, the prospect of identifying stars likely to host planets, perhaps even terrestrial planets, purely from their detailed chemical compositions is certainly enthralling.

While the link with planet formation appears secure, the connection between the abundance correlation with dust condensation and existence of planets is not yet fully established, since for the majority of the stars observed to date no planet information is at hand. It is therefore important to extend this type of extremely precise stellar abundance analysis to stars for which knowledge is available as to what planets are present as well as absent around them. We (PI=Jorge Meléndez) are currently carrying out a large program over 90 nights with the HARPS spectrograph on the ESO 3.6m telescope to search for planets around some 70 solar twins, which will also be exposed to a detailed chemical analysis using MIKE/Magellan spectra [99]. Our group is also studying in great detail Kepler stars identified to host rocky super-Earths to search for a similar chemical signature as seen in the Sun relative to solar twins (Liu et al., in preparation). For this work we analyse the Kepler stars relative to their "stellar twins", i.e. stars otherwise indistinguishable from them in terms of effective temperature, surface gravity and overall metallicity.

If indeed planet formation can imprint specific signatures in the chemical compositions of their host stars, it should be possible to identify these tell-tale signs in stars born from the same well-mixed environment but where planet formation may have proceeded differently for whatever reason. Two such types of objects are stellar binaries and open clusters. Ramírez et al. [101] did not find a similar striking signature as in Fig. 11 when analysing the 16 Cygni binary star but uncovered a general 0.04 dex difference between the two stellar components for most elements; component B which hosts a Jupiter-mass planet is slightly metal-poor [but see 102, for a contrary view]. More recently, Tucci Maia et al. [103] revisited the issue using even better spectra of the system and indeed discovered a small but significant trend with condensation temperature: the abundance differences are larger for refractory elements, in line with the general scenario suggested by Meléndez et al. [94]. Tucci Maia et al. [103] speculated that the giant planet in 16 Cygni B have a $\sim 5\,M_{\oplus}$ rocky core giving rise to the particular chemical differences between the two stars. On the other hand, Liu et al. [100] did not find any appreciable abundance differences between the two components in the HAT-P-1 binary system, in which the fainter star harbours a giant planet (Fig. 12). Clearly the situation is not as clear-cut: the
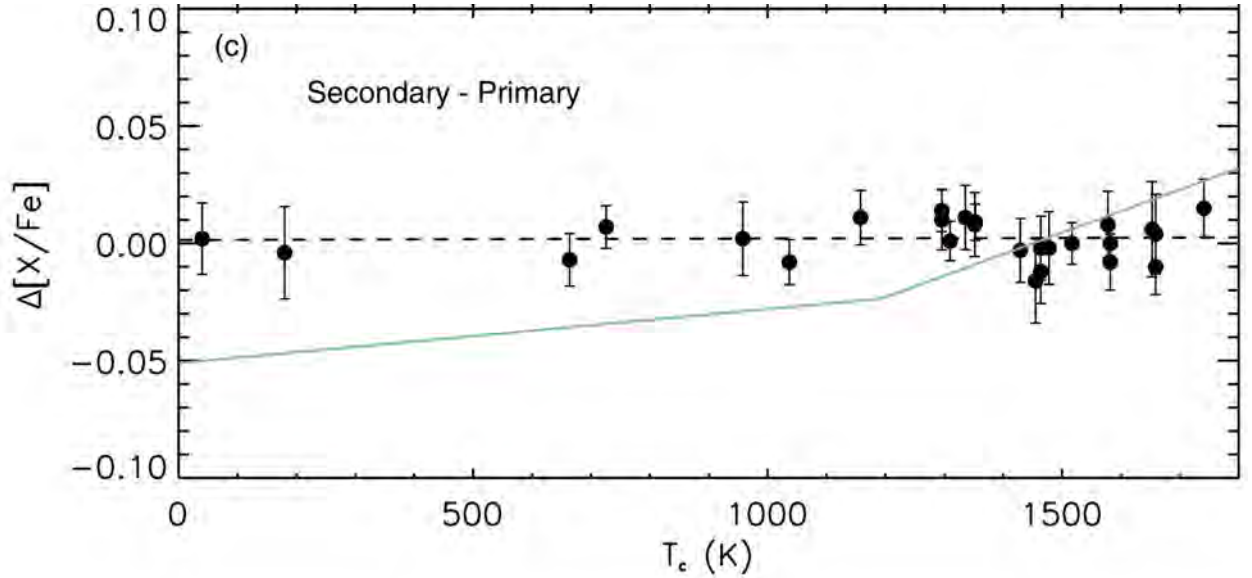
FIGURE 12. Abundance differences between the two components in the HAT-P-1 stellar binary in which the fainter secondary star hosts a gas giant planet [100].

formation of giant planets does not automatically lead to chemical differences as it depends on a range of variables, including how many and large planets formed, when the planet formation and dust-depleted accretion took place and the mass of the stars and thus the mass of the convective envelope during the pre-main sequence evolution.

In the case of open clusters, Önehag et al. [104] did not find any particular abundance variations between the observed solar twins in M67 that could be attributable to planet formation. Similarly, Liu et al. (in preparation) could not identify any planet formation signature in the Hyades open cluster. Before firm conclusions can be drawn further open clusters must be studied, striving for the highest possible precision in the abundance analysis to search for these very subtle chemical fingerprints.

OLD, ANAEMIC STARS: THE FIRST STARS IN THE UNIVERSE

The very first stars likely formed $\sim 100 - 200\,$Myr after the Big Bang in relatively small dark-matter halos [e.g. 105, and references therein]. Their births heralded a new era in the cosmos by producing not only the radiation responsible for re-ionising the Universe once again but also the first elements heavier than lithium, the first step of the cosmic chemical evolution that eventually led to planets and life. Tremendous efforts are currently dedicated to the study of the epoch of reionization and the first stars and galaxies, including being a major driver for the next generation of astronomical facilities (e.g. JWST, ELTs, SKA). There are two complementary approaches to learn about this exciting era: study galaxies at high-redshift (sometimes referred to as far-field cosmology) or ancient stars in our Galactic neighbourhood (near-field cosmology). Our telescopes are not yet powerful enough to discern the first generations of stars in the far-away Universe but we have ample examples of extremely old stars nearby, some of which may be among the oldest surviving stars to the present-day.

I will here focus on this second, near-field cosmology approach. There are a huge number of fascinating topics that could and should be covered, yet I have to be selective due to page- and time-limitations. I will not provide a detailed discussion of the nature of the first stars and their evolution and nucleosynthesis except in the context of one particular star we have recently discovered [e.g. 106]. The origin of the neutron capture elements and the possibility to radioactively date (cosmochronology) some Galactic halo stars that are heavily enriched in *r*-process elements [e.g. 107, 108] will not be covered nor will the large number of C-enhanced metal-poor stars [e.g. 109]. The recent claims of a dual Galactic halo will not be scrutinised [110, 111, 112, 113] nor will the possible connection between the Galactic halo, globular clusters and dwarf galaxies be discussed [e.g. 114]. Instead in this section I will briefly focus on just two particular topics relevant for spectroscopy: the Li abundance in extremely metal-poor stars to probe Big Bang
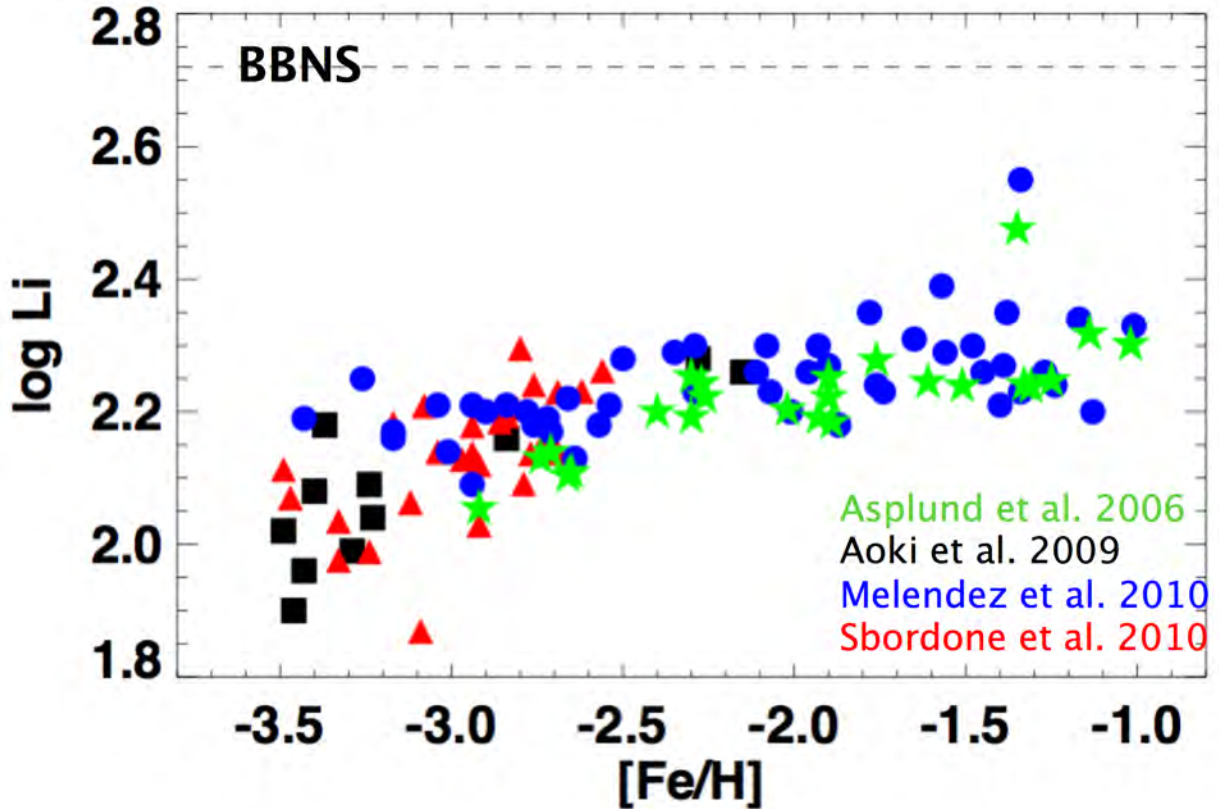
FIGURE 13. Evolution of ^{7}Li abundances in metal-poor halo turn-off stars as a function of metallicity from a few recent studies: Asplund et al. [2] (green stars), Aoki et al. [115] (black squares), Sbordone et al. [53] (red triangles) and Meléndez et al. [116] (blue circles). The dashed line denotes the predicted Li abundance from standard Big Bang nucleosynthesis.

nucleosynthesis, stellar physics and perhaps particle physics beyond the standard model and if any of the very first stars have survived to the present-day and if so where should one search for them.

Lithium in the early Universe

During the first few minutes after the Big Bang, the temperature and density were sufficiently high to produce the isotopes of the light elements hydrogen, helium and lithium. In standard Big Bang nucleosynthesis (BBNS) the exact abundance ratios of these isotopes depend only on one variable: the baryon density of the Universe. The overall agreement between predictions and observations of ^{4}He, ^{3}He, D and ^{7}Li is some of the oldest and most metal-poor galaxies, H II regions and stars have indeed been one of the pillars of the Big Bang theory. More recently however it has become possible to determine much more accurately the baryon density from anisotropies in the cosmic microwave background. It is then possible to check for consistency in our standard cosmological picture. Indeed the baryon density inferred from ^{4}He and D is in good agreement with the CMB evidence (the observational data for ^{3}He is too uncertain to set strong constraints). However there is problem with Li as measured in the oldest and most metal-poor stars in the Galactic halo in the sense that the observed value is significantly less than the BBNS prediction: the cosmological ^{7}Li problem.

Spite and Spite [1] were the first to discover the presence of Li in halo stars. They deduced an abundance which has stood the test of time remarkably well in spite of major advances in the modelling of stellar atmospheres and spectral line formation. Fig. 13 summarises a selection of more recent work [2, 115, 53, 116] in determining Li abundances in halo dwarfs and turn-off stars (subgiants and red giants have destroyed large fraction of their surface Li and thus do not reflect the primordial value). It is clear that at the lowest metallicities, the observed Li abundances are a factor of ~ 3
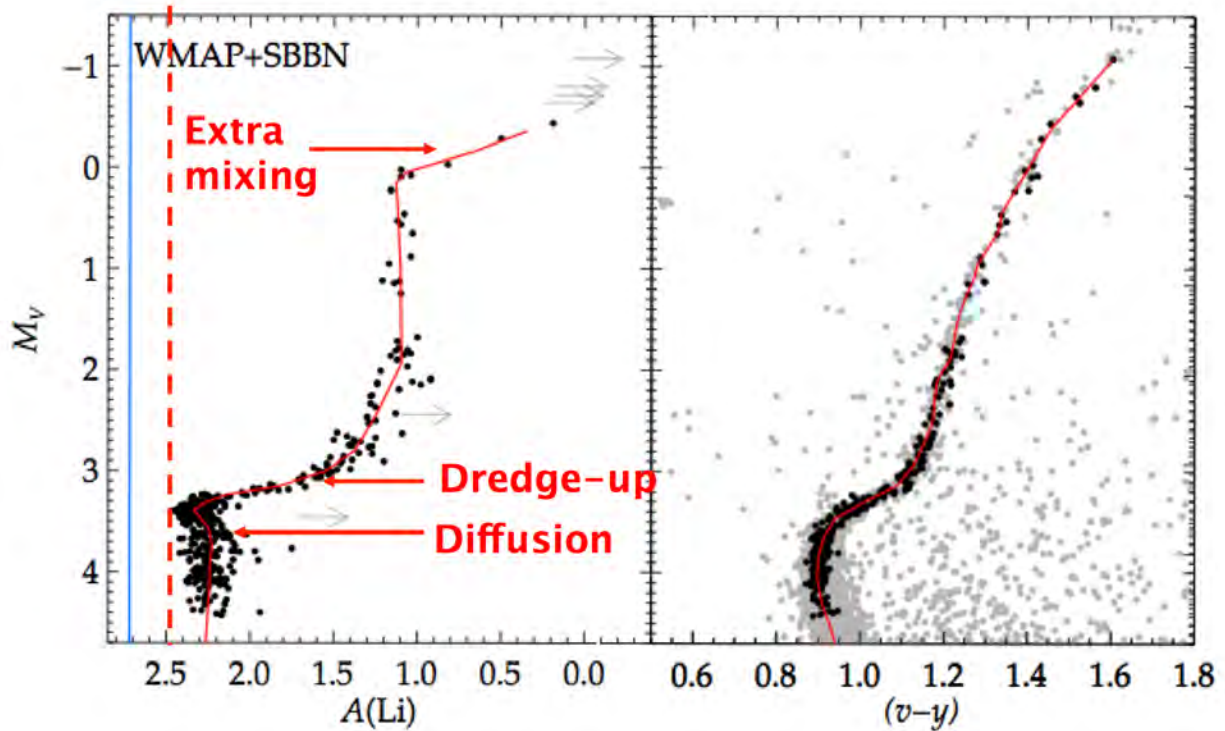
FIGURE 14. Inferred Li abundances (left panel) and observed colour magnitude diagram (right panel) of the globular cluster NGC6397 [119]. The black dots correspond to stars observed spectroscopically with VLT to enable a Li abundance determination. The photospheric Li abundances increase slightly with luminosity immediately before the first-dredge up, an increase which has been attributed to the restoration to the surface of Li removed from the convection zone by the combined effects of atomic diffusion and turbulent mixing during the main-sequence and turn-off evolution [120, 121, 119]. The blue vertical line in the left panel corresponds to the predicted primordial Li abundance from standard BBNS while the red dashed line denotes the inferred original Li abundance after accounting for diffusion and turbulence. It does not solve the entire cosmological ^{7}Li problem but it goes roughly halfway.

lower than the BBNS prediction, a result that is very robust and present also in all other similar studies. In addition, there are a number of still debated questions, including whether this so-called Spite plateau is indeed a plateau or whether it has a slope due to for example Li production in the early Galaxy or systematic errors in the analysis. Some studies argue that the plateau breaks down for [Fe/H]< -3 where the scatter becomes large, which perhaps is consistent with the fact that the two most iron-deficient turn-off stars/subgiants with [Fe/H]~ -5 have undetectable lithium ($\log$ Li ≤ 1.0). At higher [Fe/H] the intrinsic scatter in Li abundance is tiny, indeed Asplund et al. [2] argued that the observed scatter is fully compatible with the observational errors [see also 117, for early, similar claims]. The picture is complicated by the presence of a few ultra-Li deficient stars, which however may be merger products and thus not appropriate for inferring the primordial Li content [118].

What could be the explanation for this cosmological ^{7}Li problem? Possible solutions can be of stellar, cosmological, nuclear or particle nature. A nuclear explanation to the cosmological ^{7}Li problem is quite unlikely at this stage given that the relevant nuclear reactions are relatively few and they have all well-determined cross-sections. There is an abundance of proposed solutions invoking non-standard particle physics that could have impacted Big Bang nucleosynthesis. For example the presence of various postulated supersymmetric particles with the right properties (mass, lifetimes etc) and abundance could change the resulting light element abundances through their decay, annihilations or modifications of reaction rates. While exciting such suggestions are by necessity speculative without firm backing from other independent empirical evidence.

Another possibility is of course that shortcomings in the analysis techniques lead to underestimated Li abundances. The T_{eff}-scale of metal-poor stars have been notoriously uncertain for a long time, yet to bridge the discrepancy with predictions would require unrealistically large errors, on the order of 700 K. While no consensus has yet emerged

what the true $T_{\rm eff}$-scale is, most spectroscopic and photometric methods now agree to within $\sim 200\,{\rm K}$ on average (but often with much larger differences for individual stars) and thus this is highly unlikely to be the explanation. Early on, a major concern was the assumptions made in the construction of model atmospheres and line formation, i.e. 1D hydrostatic models and LTE radiative transfer. Those worries have now been alleviated by full 3D non-LTE spectral line formation calculations [42]. Incidentally the effects of 3D hydrodynamical model atmospheres [14] is almost exactly cancelled by departures from LTE [42] in the case of Li, a remarkable and depressing coincidence for those of us having spent a considerable amount of time developing the necessary computational tools to enable 3D non-LTE calculations with the goal of investigating the primordial Li abundance.

A more plausible stellar explanation would be that the current surface Li abundances do not reflect the initial Li content the stars were born with. Standard models of stellar evolution do not predict appreciable depletion of Li for metal-poor turn-off stars as the convection zone is not deep enough to reach Li-burning temperatures. However the same is true for the Sun yet the solar photospheric Li abundance is far lower than the meteoritic value, demonstrating that the Sun has destroyed most of its Li. There are plenty of proposed hydrodynamical processes that could cause additional mixing below the convection zone, including rotation [e.g. 122], gravity waves [e.g. 77] and diffusion [120], but none can be predicted from first principles and instead require parametrisation. It is however possible to constrain such models empirically using the fact that globular cluster stars should have been born with the same Li content, ignoring for the moment complications arising from multiple stellar populations and their possible Li production/destruction. Korn et al. [121] first demonstrated that turn-off stars in the cluster NGC6397 do not all share the same Li abundances, interpreting the differences as the effects of diffusion moderated by turbulent mixing that would bring the observations into rough agreement with BBNS predictions. Fig. 14 shows the results from a follow-up study of the same cluster by Lind et al. [119] with the tell-tale Li variations with stellar luminosity. Immediately before the first dredge-up the Li abundances increase slightly where the Li diffused out of the convection zone and stored immediately below is mixed back to the surface by the deepening convection zone. An empirical calibration of the diffusion plus turbulence models of Richard et al. [120] reveals that the initial Li abundance was about $0.2 - 0.3$ dex higher. If true also for the most metal-poor field stars, about half of the cosmological ^{7}Li problem could be accounted for but still requiring another effect to resolve it completely.

If stellar Li depletion is a significant part of the cosmological ^{7}Li problem, then the minor isotope ^{6}Li should for all practical purposes be undetectable in metal-poor turn-off stars as it is even more fragile. While ^{6}Li is produced in standard BBNS the amount is tiny, a factor of 1000 or so less than ^{7}Li. Still Smith et al. [123, 124] claimed the first detection of ^{6}Li in the halo star HD84937. The method relies on the isotopic shift in the Li I 670.8 nm resonance line: the exact line-shape of this unresolved feature can thus in principle reveal the ^{6}Li/^{7}Li ratio. It is an extremely challenging measurement and requires exceptionally high-quality observations ($S/N > 500$, $R \approx 100,000$). The technique is also greatly complicated by the already asymmetric line profile due to the doublet and fine structure components as well as due to the convective line asymmetries and line broadening. One must therefore first determine the intrinsic stellar broadening using otherwise simple, unblended lines, which is then applied to the Li line. In a 1D analysis this means to determine the combined macroturbulence and rotation as well as microturbulence while this simplifies to just rotational broadening in the 3D case (instrumental broadening must of course also be accounted for). Smith et al. [124] derived a value of ^{6}Li/^{7}Li$= 0.05 \pm 0.02$ for HD84937 with [Fe/H]$= -2.2$, which even without any ^{6}Li stellar depletion would be higher than the amount of ^{6}Li production from cosmic rays. Asplund et al. [2] and Asplund and Meléndez [125] extended this to many more halo stars and claimed 2σ detections in 12 additional stars, including G64-12 and LP815-43 at [Fe/H]≈ -3, far above expectations, especially when considering the small but non-negligible ^{6}Li depletion in standard stellar evolution models. This was quickly dubbed the cosmological ^{6}Li problem. It is important to note that the two cosmological Li problems are strongly coupled: most proposed solutions to bridge the ^{7}Li discrepancy such as stellar depletion tend to make the ^{6}Li problem worse and vice versa.

As already noted, measuring ^{6}Li/^{7}Li in halo turn-off stars is incredibly difficult and the inferred values must therefore be treated with caution, as also duly noted by Asplund et al. [2] and Asplund and Meléndez [125]. Cayrel et al. [126] argued that the intrinsic convective line-asymmetries can masquerade as ^{6}Li, skewing the results to too high values when not considering them properly. Furthermore, Li is sensitive to non-LTE effects, especially in the warm upflows in 3D hydrodynamical models of metal-poor stars [42]. Fig. 15). It is therefore paramount to consider both Li and the calibration lines of other elements in full 3D non-LTE, indeed a very challenging prospect. Recently, Lind et al. [3] has tackled this problem, performing 3D non-LTE calculations for Li, Na and Ca in a few metal-poor stars, including HD84937 and G64-12 using high-S/N HIRES/Keck observations (same as used by [125]). Indeed the combined effects of convection and non-LTE reduces the inferred ^{6}Li/^{7}Li ratio significantly, in the case of G64-12 completely and even for HD84937 down from ^{6}Li/^{7}Li$= 0.06 \pm 0.01$ to 0.02 ± 0.01, i.e barely a 2σ-detection (Fig. 16). Given the fundamental importance of even a single ^{6}Li detection at low [Fe/H] it is however crucial to investigate
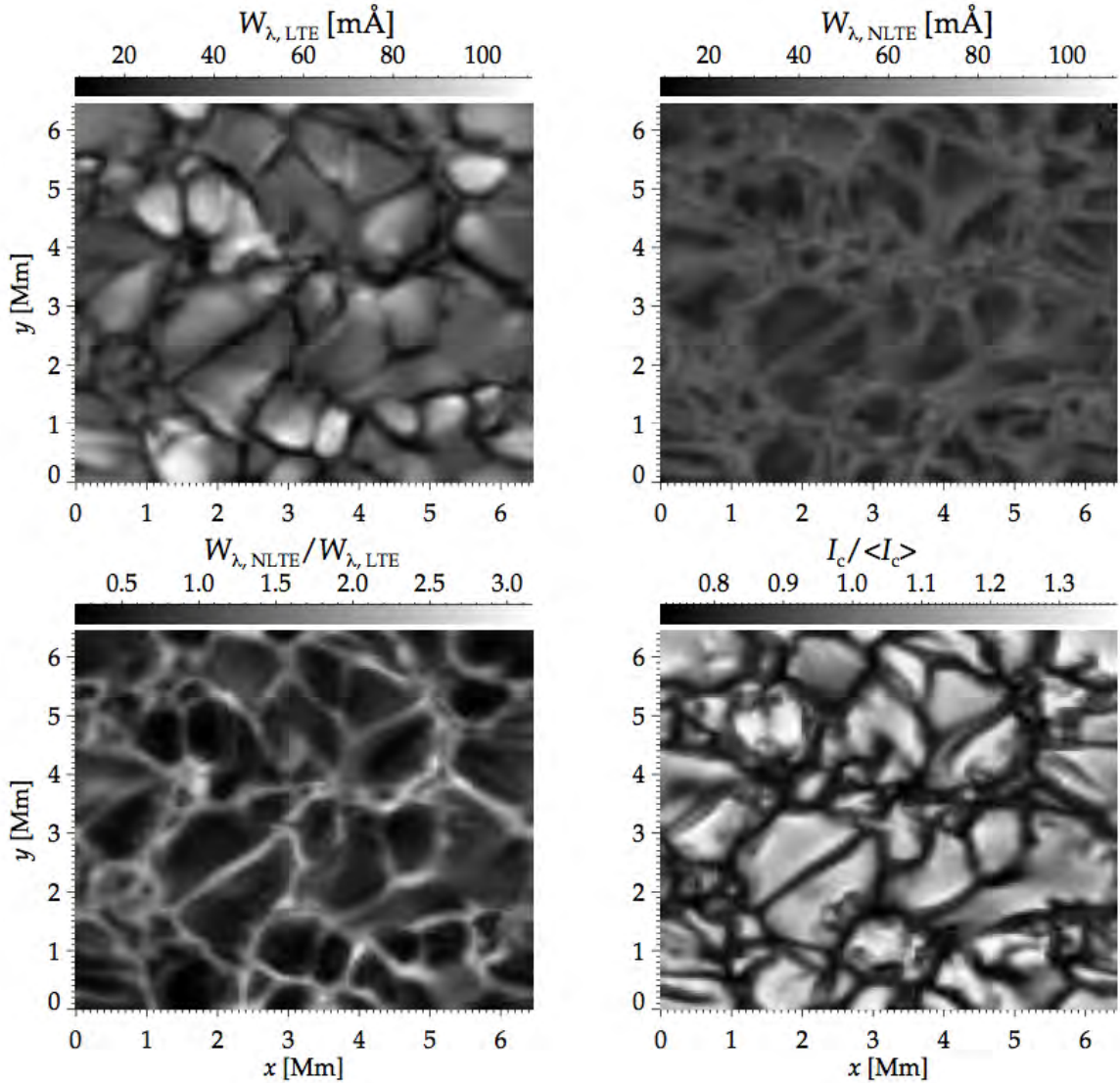
FIGURE 15. The variation of the predicted equivalent width of the Li I 670.8 nm line across the stellar surface in a 3D hydrodynamical model atmosphere of a metal-poor star [3]. In the top left the 3D LTE case is shown while the 3D non-LTE results in the upper right shows how much weaker the line becomes when allowing for departures from LTE, especially in the warm upflows. The lower panels show the ratio of the LTE and non-LTE equivalent width as well as the typical granulation pattern seen in late-type stars, here exemplified by the continuum intensities.

this further, including extending the 3D non-LTE calculations also to Fe lines, which excellent calibration lines, and to acquire even higher-quality spectra to finally resolve whether indeed ^{6}Li is present in any metal-poor turn-off star.

Where are they now?

Tremendous efforts have been made over the years to discover more extremely metal-poor stars and perhaps the first known Population III star, starting with the HK survey of Beers et al. [127] and more recently the Hamburg-ESO, SEGUE, LAMOST and SkyMapper surveys [128, 129, 130] All of these searches have targeted the Milky Way halo, which makes perfect sense as it is known to be both very old and metal-poor. By now, several hundred extremely metal-poor ([Fe/H]< -3) stars have been studied in detail with high-resolution [e.g. 131, 132] to measure

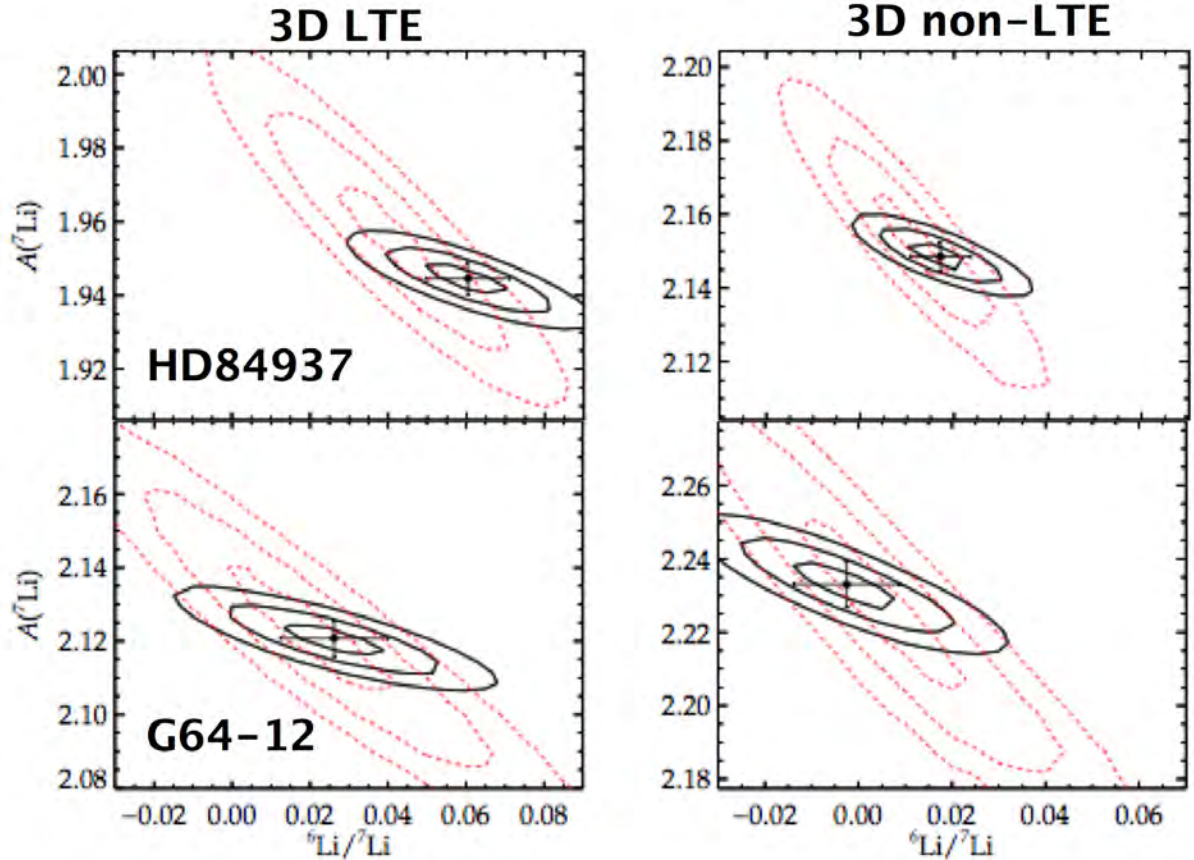**FIGURE 16.** The significance contours of the inferred ^{6}Li/^{7}Li ratios in the two metal-poor turn-off stars HD84937 (upper panel) and G64-12 (lower panel) [3]. The left column shows the results when carrying out a 3D analysis in LTE while the right column gives the full 3D non-LTE case. The black contours corresponds to the case of using calibration lines to fix the intrinsic stellar line broadening while the red contour lines denote the more restricted and more uncertain case of determining everything from the Li line itself, including the line broadening. The detections in 3D LTE turn to non-detections with a more sophisticated analysis, demonstrating the need for proper 3D non-LTE line formation calculations.

their chemical compositions to learn about nucleosynthesis in the first generations of stars and the very earliest epochs of our Milky Way. More recently, several groups have scrutinised dwarf galaxies in the Local Group as they are also among the most metal-poor stellar populations known, reaching at least down to [Fe/H]$= -4$ [133, 114]. The halo can however not have been built entirely from accretion of dwarf galaxies alike the ones which has survived to the present-day in the Local Group since their [α/Fe] ratios start decreasing to solar values at lower [Fe/H] than for halo stars.

Based on theoretical considerations, a more promising place to search for any surviving Pop. III star would be the Galactic bulge. The very first stars would have formed in the largest dark-matter over-densities at redshifts $z = 10 - 30$, which subsequently grew to become the central regions of galaxies like the Milky Way [134, 135]. Salvadori et al. [136] predicted that any star in the bulge-region with [Fe/H]< -1 would typically have formed at $z > 10$ (i.e. less than 200 million years after the Big Bang) while a corresponding halo star would have formed at $z \sim 5$. The Galactic bulge is thus of great interest in searching for the elusive Pop. III stars and their descendants. Any such search is however faced with major challenges: the bulge is predominantly metal-rich, very crowded and with high extinction/reddening. The ARGOS bulge survey found that only 0.1% of stars in the bulge have [Fe/H]< -1 [137], making any search without preselection very inefficient.
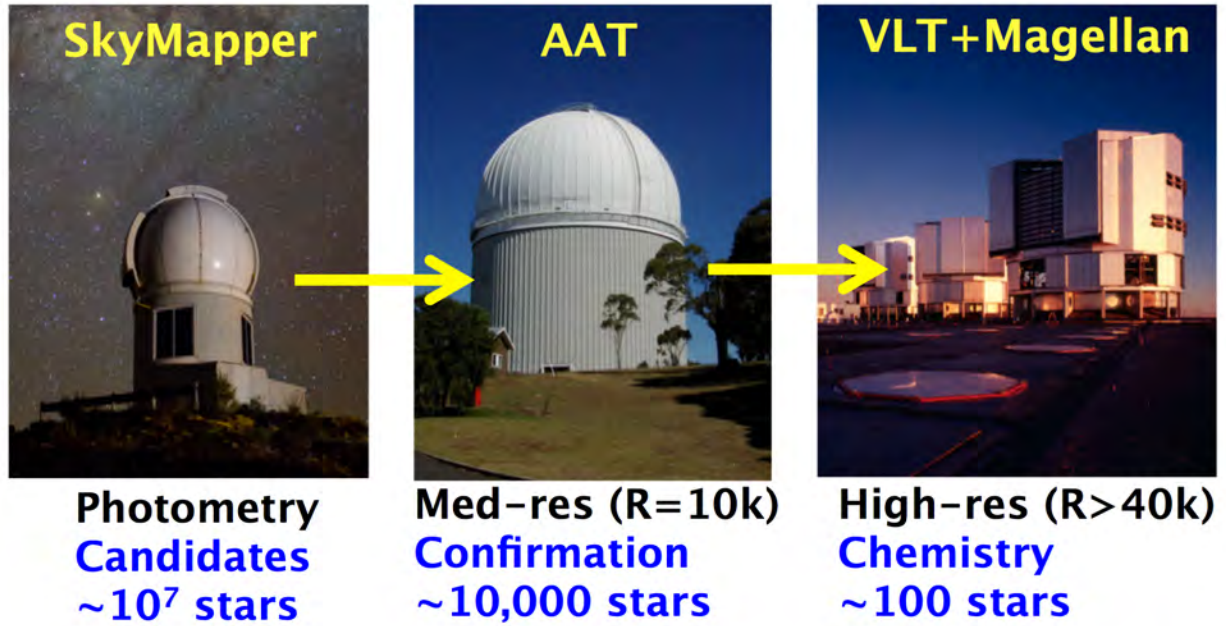
FIGURE 17. The three-pronged approach of the EMBLA survey aimed at finding extremely metal-poor stars in the Galactic bulge: photometry from the SkyMapper telescope to identify promising candidates, intermediate resolution spectroscopy with the 400 fibre AAOmega spectrograph on AAT to confirm their metal-poor status and finally high-resolution spectroscopy with VLT and Magellan to determine the chemical composition of the most interesting objects.

At the Australian National University, we have recently initiated the EMBLA[1] (Extremely Metal-poor BuLge with AAT) survey (PI=M. Asplund). The EMBLA survey has a three-pronged strategy (Fig. 17): *uvgriz* photometry from ANU's new SkyMapper telescope is used to identify promising metal-poor candidates which are then followed up with the AAOmega spectrograph on the AAT to confirm their metal-poor status by means of intermediate resolution spectroscopy before finally the most metal-poor bulge stars are observed at high resolution with Magellan and VLT to determine their detailed chemical compositions. The unique *uvgriz* SkyMapper photometry is ideal for stellar physics and Galactic archaeology, with in particular the *v* filter sensitive to metallicity as it is centred on the Ca II HK lines. Fig. 18 illustrates our selection criteria, which demonstrates how successful our approach is also for a crowded and reddened region like the bulge. Furthermore, AAOmega can observe 400 stars simultaneously over a 2-degree field-of-view, making the survey extremely efficient in terms of telescope time for identifying metal-poor stars.

Before the EMBLA survey started, only a dozen or so bulge stars were known with [Fe/H]< -2, with the most metal-poor stars observed at high-resolution having [Fe/H]$= -2.0$ [138]. As Fig. 19 shows, from the 10,000 stars observed with AAOmega we have discovered a whole host of very metal-poor stars, including > 100 stars with [Fe/H]< -3. The first high-resolution analysis of four bulge stars observed in 2012 as part of the Gaia-ESO survey [139] with VLT have recently been completed (Howes et al., in preparation), including a star with [Fe/H]$= -2.8$. Since then we have observed a further ~ 30 bulge stars, including one exciting star with [Fe/H]$= -4$ (Howes et al., in preparation). If the theoretical expectations are correct, these stars are excellent candidates to be extremely old, having formed at redshifts $z > 10$. If so, it would make them the oldest known objects in the Universe, probing an era not accessible in any other way. Since they have a finite metal-content they are still not true first stars but a second (or possibly later) generation star. Their detailed chemistry can however reveal the nature of their ancestors. Overall, the few stars analysed have much in common in terms of abundances with halo stars of similar metallicity. A detailed comparison will however have to await a much larger sample, which fortunately is underway through the EMBLA survey. A detailed study of the kinematics of these stars is important to disentangle stars always residing in the bulge as expected for the very earliest generations of stars with halo star interlopers currently passing through the bulge.

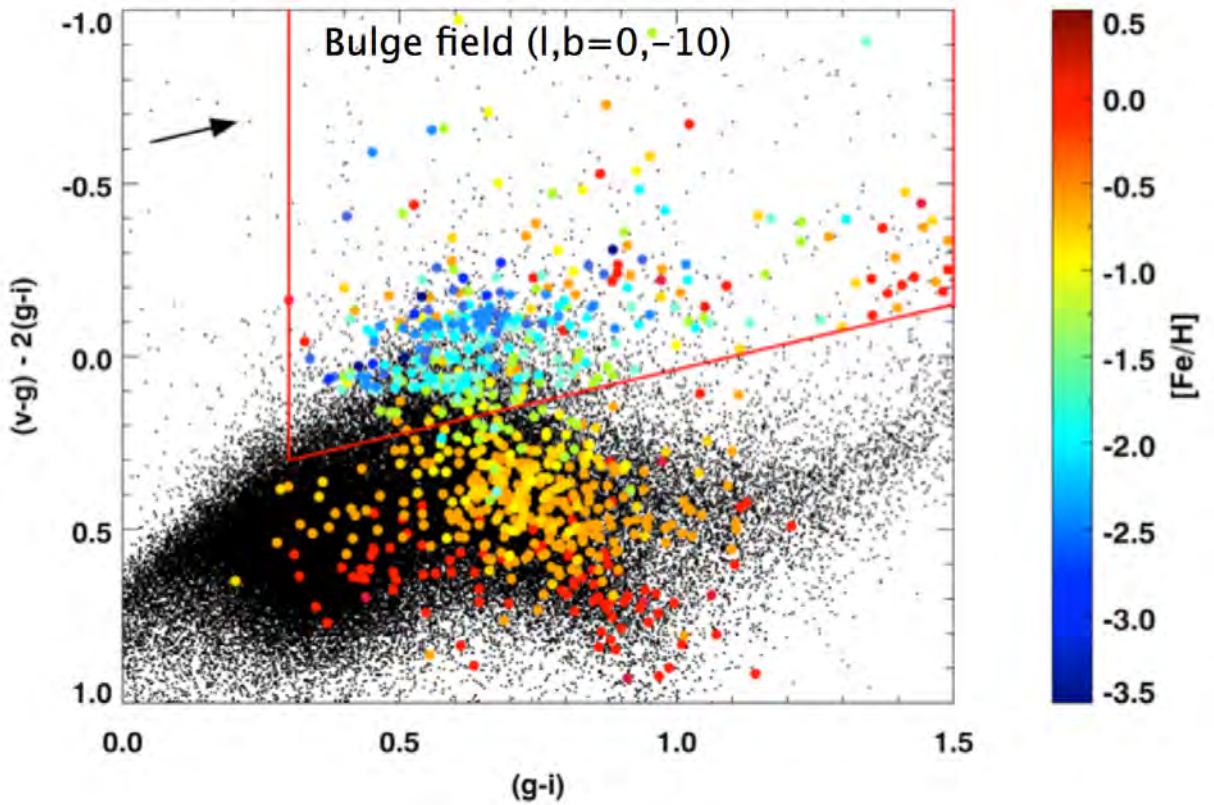[1] In Nordic mythology Embla was the first woman, born in the middle of the Universe from remnants of giants.

FIGURE 18. The colour-colour selection criteria (red lines) of the EMBLA survey to identify metal-poor bulge stars using SkyMapper *uvgriz* photometry (black dots). Also shown are stars observed with AAOmega/AAT in this particular bulge field $(l, b = 0, -10)$, colour-coded in their spectroscopically inferred metallicities. As can be seen, metal-poor stars cluster in the adopted selection box with only a relatively small level of contamination of metal-rich stars, mostly due to blends in the photometry and high reddening.

With SkyMapper we also have a program aimed at finding extremely metal-poor stars in the Galactic halo, which follows much the same strategy as the bulge survey except that the confirmation step with intermediate resolution spectroscopy is done one star at a time with ANU's 2.3m telescope and the WiFeS spectrograph as the halo stars are spread over the entire sky. No doubt the most exciting result so far from the halo program is the discovery of the most iron-deficient star ever found: SMSS J031300.362 − 670839.3 [5]. In fact, there are no discernible iron lines whatsoever in our MIKE/Magellan spectrum of this red giant branch star, with only a remarkable upper limit to be placed: [Fe/H]< -7.1. Atomic lines of only three elements are detected: Li, Mg and Ca. The star is however extremely C-rich with [C/H]$= -2.6$; a new high-S/N UV spectrum obtained with UVES/VLT also reveal the presence of many OH lines, revealing that the star is also very O-rich (Bessell et al., in preparation).

Until recently, the expectation was that the first stars were systematically all very massive, $M > 100 \, \mathrm{M}_\odot$ or so [105]. If so, none would obviously have survived to the present-day. More recently however improved numerical simulations of the formation of the first stars have demonstrated that fragmentation is important and thus low mass stars can also form [140, 141]; whether any stars formed with $M < 0.8 \, \mathrm{M}_\odot$ required to survive until today remains to be seen. Given its remarkably low iron content but presence of at least some other elements, SMSS J031300.362 − 670839.3 must have been produced from the ashes of just a single supernovae. Its abundance pattern is not consistent with nucleosynthesis in a pair-instability supernovae of a very massive star. Instead its chemistry can be rather well reproduced from a low-energetic supernovae from a moderately massive ($M \sim 60 \, \mathrm{M}_\odot$) star with a strong fall-back into the newly formed black hole (Fig. 20). We naturally hope to discover more of these exciting objects, both in the halo and in the bulge, through the SkyMapper program.
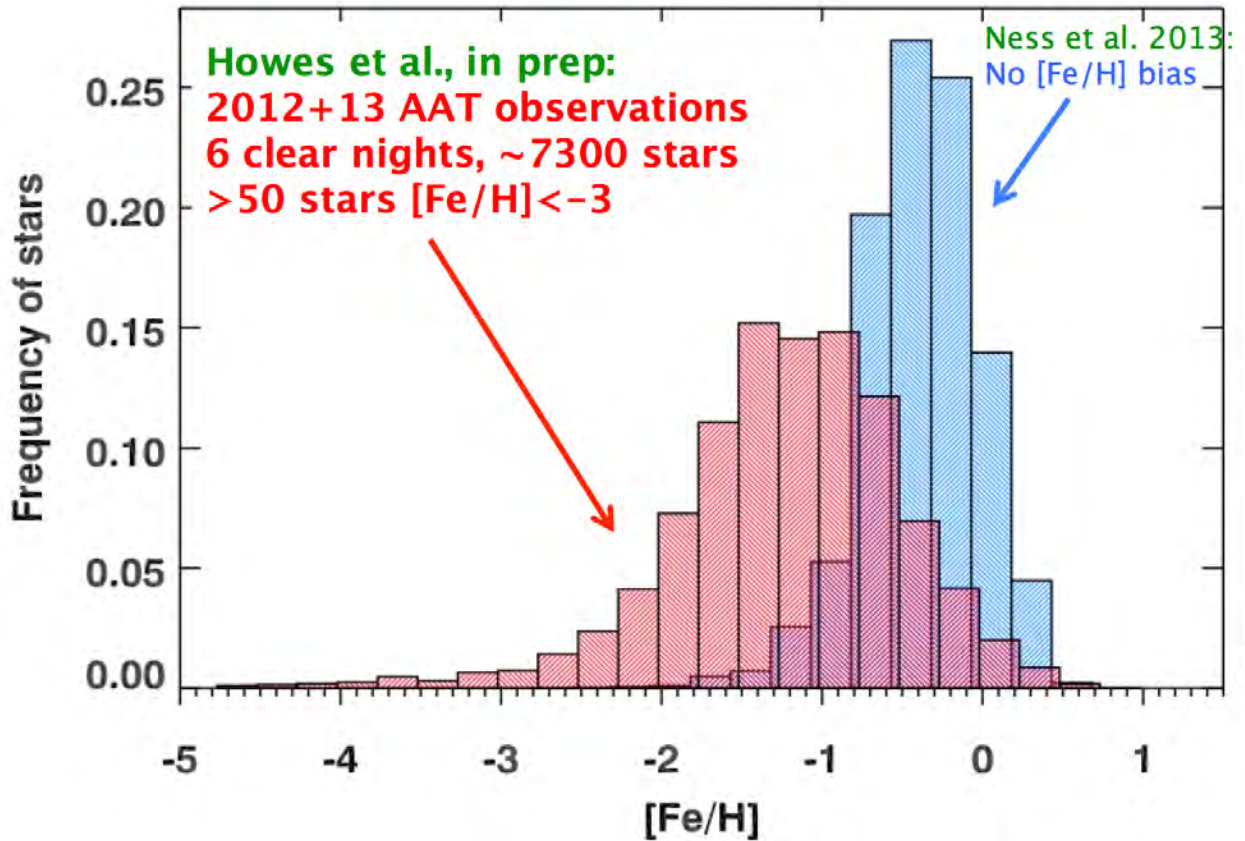
FIGURE 19. The observed bulge metallicity distribution function of the unbiased ARGOS survey [137] and the EMBLA survey (Howes et al. 2014) aimed at finding extremely metal-poor stars in the Galactic bulge; in both cases the metallicities are inferred from intermediate resolution spectroscopy using AAOmega/AAT. Since the EMBLA survey relies on SkyMapper *uvgriz* photometry to preselect metal-poor stars it has severe selection biases at high metallicity but it demonstrates the feasibility to identify even extremely metal-poor stars in the Galactic bulge, including > 100 stars with [Fe/H]< -3

CONCLUDING REMARKS

The field of stellar spectroscopy plays a central role in modern astrophysics and cosmology with most of our understanding of the Universe stemming from star-light one way or another. Of special relevance is the determination of stellar chemical compositions – the make-up of stars – which can probe cosmic, galactic, stellar and planetary evolution. In this review I have tried to provide a taste for different possible applications, covering from the Sun and the chemical imprints of planet formation in stars to the very first star born after the Big Bang; needless to say, there is an enormous wealth of other topics of similar importance I could have chosen to discuss. I have also given a brief description of recent advances the necessary theoretical tools in this field: the construction of stellar model atmospheres and how to compute the emergent stellar radiation. The field of stellar spectroscopy is currently undergoing a transformation to a time where 3D MHD stellar atmospheres and non-LTE spectral line formation will be common-place, placing all results on a much firmer theoretical footing. We are truly entering the era of precision stellar spectroscopy.
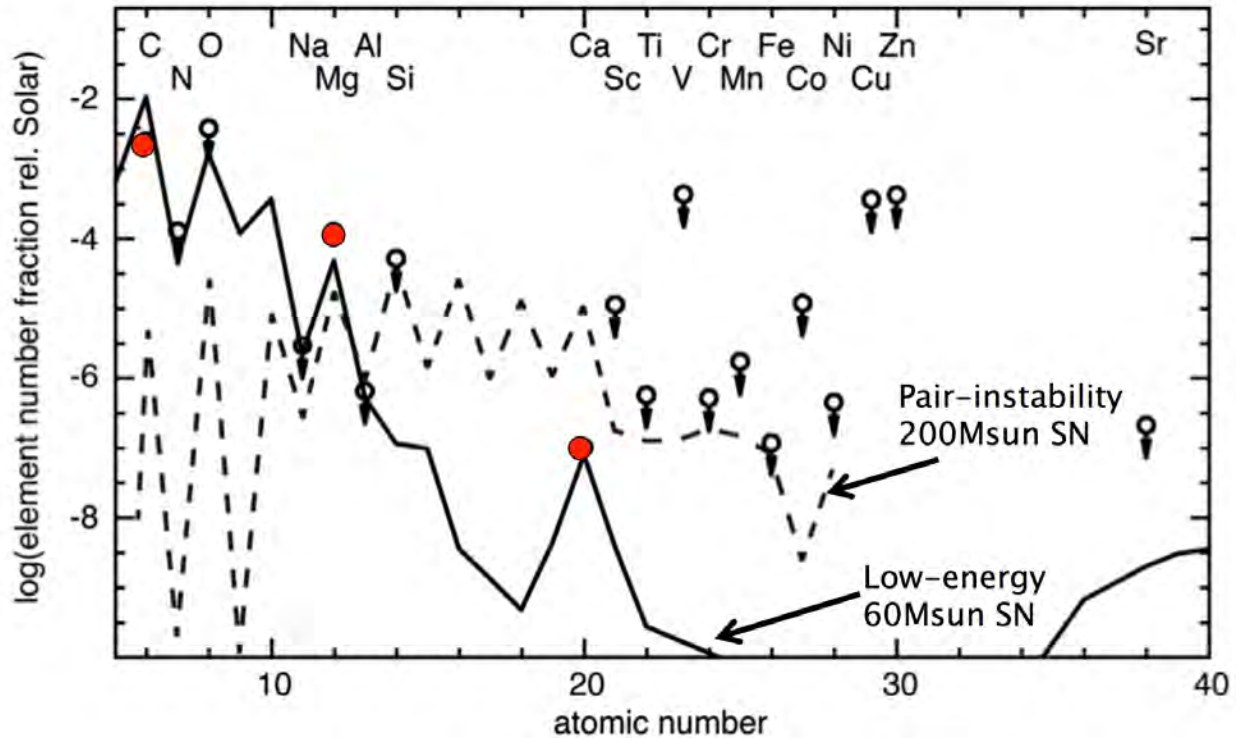
ACKNOWLEDGMENTS

FIGURE 20. The observed abundance pattern of the most iron-deficient star ever discovered, SMSS J031300.362 − 670839.3 (red circles=measurements, open circles with arrows=upper limits) [5]. Also shown are predictions for a Pop. III pair-instability supernovae (dashed line) and a low-energetic supernovae of a less massive star ($M = 60\,\mathrm{M_\odot}$).

REFERENCES

1. M. Spite, and F. Spite, *Nature* **297**, 483–485 (1982).
2. M. Asplund, D. L. Lambert, P. E. Nissen, F. Primas, and V. V. Smith, *ApJ* **644**, 229–259 (2006), `astro-ph/0510636`.
3. K. Lind, J. Melendez, M. Asplund, R. Collet, and Z. Magic, *A&A* **554**, A96 (2013), `1305.6564`.
4. K. Freeman, and J. Bland-Hawthorn, *ARA&A* **40**, 487–537 (2002), `astro-ph/0208106`.
5. S. C. Keller, M. S. Bessell, A. Frebel, A. R. Casey, M. Asplund, H. R. Jacobson, K. Lind, J. E. Norris, D. Yong, A. Heger, Z. Magic, G. S. da Costa, B. P. Schmidt, and P. Tisserand, *Nature* **506**, 463–466 (2014), `1402.1517`.
6. B. Gustafsson, R. A. Bell, K. Eriksson, and A. Nordlund, *A&A* **42**, 407–432 (1975).
7. B. Gustafsson, B. Edvardsson, K. Eriksson, U. G. Jørgensen, Å. Nordlund, and B. Plez, *A&A* **486**, 951–970 (2008), `0805.0554`.
8. R. L. Kurucz, *ApJS* **40**, 1–340 (1979).
9. E. Böhm-Vitense, *ZAp* **46**, 108 (1958).
10. Å. Nordlund, R. F. Stein, and M. Asplund, *Living Reviews in Solar Physics* **6**, 2 (2009).
11. Z. Magic, R. Collet, M. Asplund, R. Trampedach, W. Hayek, A. Chiavassa, R. F. Stein, and Å. Nordlund, *A&A* **557**, A26 (2013), `1302.2621`.
12. A. Nordlund, and D. Dravins, *A&A* **228**, 155–217 (1990).
13. H.-G. Ludwig, B. Freytag, and M. Steffen, *A&A* **346**, 111–124 (1999), `astro-ph/9811179`.

14. M. Asplund, Å. Nordlund, R. Trampedach, and R. F. Stein, *A&A* **346**, L17–L20 (1999), `astro-ph/9905059`.
15. S. Shelyag, M. Schüssler, S. K. Solanki, S. V. Berdyugina, and A. Vögler, *A&A* **427**, 335–343 (2004).
16. R. Collet, M. Asplund, and R. Trampedach, *ApJ* **644**, L121–L124 (2006), `astro-ph/0605219`.
17. B. Beeck, R. Collet, M. Steffen, M. Asplund, R. H. Cameron, B. Freytag, W. Hayek, H.-G. Ludwig, and M. Schüssler, *A&A* **539**, A121 (2012), `1201.1103`.
18. R. Trampedach, M. Asplund, R. Collet, Å. Nordlund, and R. F. Stein, *ApJ* **769**, 18 (2013), `1303.1780`.
19. A. Nordlund, *A&A* **107**, 1–10 (1982).
20. R. F. Stein, and Å. Nordlund, *ApJ* **499**, 914–933 (1998).
21. B. Freytag, M. Steffen, H.-G. Ludwig, S. Wedemeyer-Böhm, W. Schaffenberger, and O. Steiner, *Journal of Computational Physics* **231**, 919–959 (2012), `1110.6844`.
22. K. Galsgaard, and Å. Nordlund, *J. Geophys. Res.* **101**, 13445–13460 (1996).
23. Z. Magic, R. Collet, and M. Asplund, *ArXiv e-prints* (2014), `1403.6245`.
24. Z. Magic, A. Weiss, and M. Asplund, *ArXiv e-prints* (2014), `1403.1062`.
25. T. M. D. Pereira, M. Asplund, R. Collet, I. Thaler, R. Trampedach, and J. Leenaarts, *A&A* **554**, A118 (2013), `1304.4932`.
26. H. Holweger, and E. A. Mueller, *Sol. Phys.* **39**, 19–30 (1974).
27. M. Asplund, N. Grevesse, A. J. Sauval, and P. Scott, *ARA&A* **47**, 481–522 (2009), `0909.0948`.
28. M. Carlsson, R. F. Stein, Å. Nordlund, and G. B. Scharmer, *ApJ* **610**, L137–L140 (2004), `astro-ph/0406160`.
29. M. Rempel, M. Schüssler, R. H. Cameron, and M. Knölker, *Science* **325**, 171– (2009), `0907.2259`.
30. M. Rempel, *ApJ* **789**, 132 (2014), `1405.6814`.
31. B. Beeck, M. Schüssler, and A. Reiners, *ArXiv e-prints* (2014), `1408.1802`.
32. R. Trampedach, R. F. Stein, J. Christensen-Dalsgaard, Å. Nordlund, and M. Asplund, *MNRAS* **442**, 805–820 (2014), `1405.0236`.
33. M. Asplund, *ARA&A* **43**, 481–530 (2005).
34. M. Asplund, Å. Nordlund, R. Trampedach, C. Allende Prieto, and R. F. Stein, *A&A* **359**, 729–742 (2000), `astro-ph/0005320`.
35. T. M. D. Pereira, M. Asplund, and D. Kiselman, *A&A* **508**, 1403–1416 (2009), `0909.2310`.
36. D. Dravins, and A. Nordlund, *A&A* **228**, 184 (1990).
37. C. Allende Prieto, D. L. Lambert, and M. Asplund, *ApJ* **556**, L63–L66 (2001), `astro-ph/0106360`.
38. N. Shchukina, and J. Trujillo Bueno, *ApJ* **550**, 970–990 (2001).
39. H.-G. Ludwig, E. Caffau, M. Steffen, P. Bonifacio, and L. Sbordone, *A&A* **509**, A84 (2010), `0911.4251`.
40. E. Caffau, H.-G. Ludwig, M. Steffen, B. Freytag, and P. Bonifacio, *Sol. Phys.* **268**, 255–269 (2011), `1003.1190`.
41. E. Caffau, P. Bonifacio, P. François, M. Spite, F. Spite, S. Zaggia, H.-G. Ludwig, M. Steffen, L. Mashonkina, L. Monaco, L. Sbordone, P. Molaro, R. Cayrel, B. Plez, V. Hill, F. Hammer, and S. Randich, *A&A* **542**, A51 (2012), `1203.2607`.
42. M. Asplund, M. Carlsson, and A. V. Botnen, *A&A* **399**, L31–L34 (2003), `astro-ph/0302406`.
43. H.-W. Drawin, *Zeitschrift fur Physik* **211**, 404–417 (1968).
44. H. W. Drawin, *Zeitschrift fur Physik* **225**, 483–493 (1969).
45. D. Fabbian, M. Asplund, P. S. Barklem, M. Carlsson, and D. Kiselman, *A&A* **500**, 1221–1238 (2009), `0902.4472`.
46. K. Lind, M. Asplund, and P. S. Barklem, *A&A* **503**, 541–544 (2009), `0906.0899`.
47. L. Mashonkina, A. J. Korn, and N. Przybilla, *A&A* **461**, 261–275 (2007), `astro-ph/0609527`.
48. L. Mashonkina, T. Gehren, J.-R. Shi, A. J. Korn, and F. Grupp, *A&A* **528**, A87 (2011), `1101.4570`.
49. M. Bergemann, *MNRAS* **413**, 2184–2198 (2011), `1101.0828`.
50. M. Bergemann, R.-P. Kudritzki, B. Plez, B. Davies, K. Lind, and Z. Gazak, *ApJ* **751**, 156 (2012), `1204.0511`.
51. D. Kiselman, *ApJ* **489**, L107–L110 (1997), `astro-ph/9708198`.
52. H. Uitenbroek, *ApJ* **498**, 427–440 (1998).
53. L. Sbordone, P. Bonifacio, E. Caffau, H.-G. Ludwig, N. T. Behara, J. I. González Hernández, M. Steffen, R. Cayrel, B. Freytag, C. van't Veer, P. Molaro, B. Plez, T. Sivarani, M. Spite, F. Spite, T. C. Beers, N. Christlieb, P. François, and V. Hill, *A&A* **522**, A26 (2010), `1003.4510`.
54. M. Asplund, N. Grevesse, A. J. Sauval, C. Allende Prieto, and D. Kiselman, *A&A* **417**, 751–768 (2004), `astro-ph/0312290`.
55. M. Bergemann, K. Lind, R. Collet, Z. Magic, and M. Asplund, *MNRAS* **427**, 27–49 (2012), `1207.2455`.
56. P. Scott, N. Grevesse, M. Asplund, A. J. Sauval, K. Lind, Y. Takeda, R. Collet, R. Trampedach, and W. Hayek, *ArXiv e-prints* (2014), `1405.0279`.
57. P. Scott, M. Asplund, N. Grevesse, M. Bergemann, and A. J. Sauval, *ArXiv e-prints* (2014), `1405.0287`.
58. E. Anders, and N. Grevesse, *Geochim. Cosmochim. Acta* **53**, 197–214 (1989).
59. N. Grevesse, and A. J. Sauval, *Space Sci. Rev.* **85**, 161–174 (1998).
60. K. Lodders, *ApJ* **591**, 1220–1247 (2003).
61. M. Asplund, N. Grevesse, and A. J. Sauval, "The Solar Chemical Composition," in *Cosmic Abundances as Records of Stellar Evolution and Nucleosynthesis*, edited by T. G. Barnes, III, and F. N. Bash, 2005, vol. 336 of *Astronomical Society of the Pacific Conference Series*, p. 25.
62. K. Lodders, H. Palme, and H.-P. Gail, *Landolt Börnstein* p. 44 (2009), `0901.1149`.
63. N. Grevesse, P. Scott, M. Asplund, and A. J. Sauval, *ArXiv e-prints* (2014), `1405.0288`.
64. J. Meléndez, and M. Asplund, *A&A* **490**, 817–821 (2008), `0808.2796`.

65. E. Caffau, H.-G. Ludwig, M. Steffen, T. R. Ayres, P. Bonifacio, R. Cayrel, B. Freytag, and B. Plez, *A&A* **488**, 1031–1046 (2008), `0805.4398`.
66. E. Caffau, H.-G. Ludwig, J.-M. Malherbe, P. Bonifacio, M. Steffen, and L. Monaco, *A&A* **554**, A126 (2013), `1305.1763`.
67. D. L. Lambert, *MNRAS* **182**, 249–271 (1978).
68. S. Johansson, U. Litzén, H. Lundberg, and Z. Zhang, *ApJ* **584**, L107–L110 (2003), `astro-ph/0301382`.
69. E. Caffau, E. Maiorca, P. Bonifacio, R. Faraggiana, M. Steffen, H.-G. Ludwig, I. Kamp, and M. Busso, *A&A* **498**, 877–884 (2009), `0903.3406`.
70. E. Caffau, H.-G. Ludwig, P. Bonifacio, R. Faraggiana, M. Steffen, B. Freytag, I. Kamp, and T. R. Ayres, *A&A* **514**, A92 (2010), `1002.2628`.
71. D. Fabbian, E. Khomenko, F. Moreno-Insertis, and Å. Nordlund, *ApJ* **724**, 1536–1541 (2010), `1006.0231`.
72. D. Fabbian, F. Moreno-Insertis, E. Khomenko, and Å. Nordlund, *A&A* **548**, A35 (2012), `1209.2771`.
73. F. Delahaye, and M. H. Pinsonneault, *ApJ* **649**, 529–540 (2006), `astro-ph/0511779`.
74. S. Basu, and H. M. Antia, *Phys. Rep.* **457**, 217–283 (2008), `0711.4590`.
75. A. M. Serenelli, S. Basu, J. W. Ferguson, and M. Asplund, *ApJ* **705**, L123–L127 (2009), `0909.2668`.
76. T. R. Monroe, J. Meléndez, I. Ramírez, D. Yong, M. Bergemann, M. Asplund, M. Bedell, M. Tucci Maia, J. Bean, K. Lind, A. Alves-Brito, L. Casagrande, M. Castro, J.-D. do Nascimento, M. Bazot, and F. C. Freitas, *ApJ* **774**, L32 (2013), `1308.5744`.
77. C. Charbonnel, and S. Talon, *Science* **309**, 2189–2191 (2005), `astro-ph/0511265`.
78. S. N. Nahar, A. K. Pradhan, G.-X. Chen, and W. Eissner, *Phys. Rev. A* **83**, 053417 (2011), `1104.2881`.
79. M. Mayor, and D. Queloz, *Nature* **378**, 355–359 (1995).
80. S. Udry, and N. C. Santos, *ARA&A* **45**, 397–439 (2007).
81. W. J. Borucki, D. Koch, G. Basri, N. Batalha, T. Brown, D. Caldwell, J. Caldwell, J. Christensen-Dalsgaard, W. D. Cochran, E. DeVore, E. W. Dunham, A. K. Dupree, T. N. Gautier, J. C. Geary, R. Gilliland, A. Gould, S. B. Howell, J. M. Jenkins, Y. Kondo, D. W. Latham, G. W. Marcy, S. Meibom, H. Kjeldsen, J. J. Lissauer, D. G. Monet, D. Morrison, D. Sasselov, J. Tarter, A. Boss, D. Brownlee, T. Owen, D. Buzasi, D. Charbonneau, L. Doyle, J. Fortney, E. B. Ford, M. J. Holman, S. Seager, J. H. Steffen, W. F. Welsh, J. Rowe, H. Anderson, L. Buchhave, D. Ciardi, L. Walkowicz, W. Sherry, E. Horch, H. Isaacson, M. E. Everett, D. Fischer, G. Torres, J. A. Johnson, M. Endl, P. MacQueen, S. T. Bryson, J. Dotson, M. Haas, J. Kolodziejczak, J. Van Cleve, H. Chandrasekaran, J. D. Twicken, E. V. Quintana, B. D. Clarke, C. Allen, J. Li, H. Wu, P. Tenenbaum, E. Verner, F. Bruhweiler, J. Barnes, and A. Prsa, *Science* **327**, 977– (2010).
82. N. M. Batalha, J. F. Rowe, S. T. Bryson, T. Barclay, C. J. Burke, D. A. Caldwell, J. L. Christiansen, F. Mullally, S. E. Thompson, T. M. Brown, A. K. Dupree, D. C. Fabrycky, E. B. Ford, J. J. Fortney, R. L. Gilliland, H. Isaacson, D. W. Latham, G. W. Marcy, S. N. Quinn, D. Ragozzine, A. Shporer, W. J. Borucki, D. R. Ciardi, T. N. Gautier, III, M. R. Haas, J. M. Jenkins, D. G. Koch, J. J. Lissauer, W. Rapin, G. S. Basri, A. P. Boss, L. A. Buchhave, J. A. Carter, D. Charbonneau, J. Christensen-Dalsgaard, B. D. Clarke, W. D. Cochran, B.-O. Demory, J.-M. Desert, E. Devore, L. R. Doyle, G. A. Esquerdo, M. Everett, F. Fressin, J. C. Geary, F. R. Girouard, A. Gould, J. R. Hall, M. J. Holman, A. W. Howard, S. B. Howell, K. A. Ibrahim, K. Kinemuchi, H. Kjeldsen, T. C. Klaus, J. Li, P. W. Lucas, S. Meibom, R. L. Morris, A. Prša, E. Quintana, D. T. Sanderfer, D. Sasselov, S. E. Seader, J. C. Smith, J. H. Steffen, M. Still, M. C. Stumpe, J. C. Tarter, P. Tenenbaum, G. Torres, J. D. Twicken, K. Uddin, J. Van Cleve, L. Walkowicz, and W. F. Welsh, *ApJS* **204**, 24 (2013), `1202.5852`.
83. G. Gonzalez, *MNRAS* **285**, 403–412 (1997).
84. D. A. Fischer, and J. Valenti, *ApJ* **622**, 1102–1117 (2005).
85. J. B. Pollack, O. Hubickyj, P. Bodenheimer, J. J. Lissauer, M. Podolak, and Y. Greenzweig, *Icarus* **124**, 62–85 (1996).
86. A. P. Boss, *Science* **276**, 1836–1839 (1997).
87. A. Johansen, J. S. Oishi, M.-M. Mac Low, H. Klahr, T. Henning, and A. Youdin, *Nature* **448**, 1022–1025 (2007), `0708.3890`.
88. J. C. Bond, D. P. O'Brien, and D. S. Lauretta, *ApJ* **715**, 1050–1070 (2010), `1004.0971`.
89. S. E. Robinson, G. Laughlin, P. Bodenheimer, and D. Fischer, *ApJ* **643**, 484–500 (2006), `astro-ph/0601656`.
90. G. Israelian, N. C. Santos, M. Mayor, and R. Rebolo, *Nature* **411**, 163–166 (2001).
91. G. Israelian, E. Delgado Mena, N. C. Santos, S. G. Sousa, M. Mayor, S. Udry, C. Domínguez Cerdeña, R. Rebolo, and S. Randich, *Nature* **462**, 189–191 (2009), `0911.4198`.
92. E. Delgado Mena, G. Israelian, J. I. González Hernández, S. G. Sousa, A. Mortier, N. C. Santos, V. Z. Adibekyan, J. Fernandes, R. Rebolo, S. Udry, and M. Mayor, *A&A* **562**, A92 (2014), `1311.6414`.
93. P. Baumann, I. Ramírez, J. Meléndez, M. Asplund, and K. Lind, *A&A* **519**, A87 (2010), `1008.0575`.
94. J. Meléndez, M. Asplund, B. Gustafsson, and D. Yong, *ApJ* **704**, L66–L70 (2009), `0909.2299`.
95. I. Ramírez, J. Meléndez, and M. Asplund, *A&A* **508**, L17–L20 (2009).
96. I. Ramírez, M. Asplund, P. Baumann, J. Meléndez, and T. Bensby, *A&A* **521**, A33 (2010), `1008.3161`.
97. M. Bedell, J. Melendez, J. Bean, I. Ramirez, P. Leite, and M. Asplund, *ArXiv e-prints* (2014), `1409.1230`.
98. J. E. Chambers, *ApJ* **724**, 92–97 (2010).
99. I. Ramirez, J. Melendez, J. Bean, M. Asplund, M. Bedell, T. Monroe, L. Casagrande, L. Schirbel, S. Dreizler, J. Teske, M. Tucci Maia, A. Alves-Brito, and P. Baumann, *ArXiv e-prints* (2014), `1408.4130`.
100. F. Liu, M. Asplund, I. Ramírez, D. Yong, and J. Meléndez, *MNRAS* **442**, L51–L55 (2014), `1404.2112`.
101. I. Ramírez, J. Meléndez, D. Cornejo, I. U. Roederer, and J. R. Fish, *ApJ* **740**, 76 (2011), `1107.5814`.
102. S. C. Schuler, K. Cunha, V. V. Smith, L. Ghezzi, J. R. King, C. P. Deliyannis, and A. M. Boesgaard, *ApJ* **737**, L32 (2011), `1107.3183`.

103. M. Tucci Maia, J. Meléndez, and I. Ramírez, *ApJ* **790**, L25 (2014), `1407.4132`.
104. A. Önehag, B. Gustafsson, and A. Korn, *A&A* **562**, A102 (2014), `1310.6297`.
105. V. Bromm, *Reports on Progress in Physics* **76**, 112901 (2013), `1305.5178`.
106. A. Heger, and S. E. Woosley, *ApJ* **724**, 341–373 (2010), `0803.3161`.
107. R. Cayrel, V. Hill, T. C. Beers, B. Barbuy, M. Spite, F. Spite, B. Plez, J. Andersen, P. Bonifacio, P. François, P. Molaro, B. Nordström, and F. Primas, *Nature* **409**, 691–692 (2001), `astro-ph/0104357`.
108. A. Frebel, N. Christlieb, J. E. Norris, C. Thom, T. C. Beers, and J. Rhee, *ApJ* **660**, L117–L120 (2007), `astro-ph/0703414`.
109. S. Lucatello, T. C. Beers, N. Christlieb, P. S. Barklem, S. Rossi, B. Marsteller, T. Sivarani, and Y. S. Lee, *ApJ* **652**, L37–L40 (2006), `astro-ph/0609730`.
110. D. Carollo, T. C. Beers, Y. S. Lee, M. Chiba, J. E. Norris, R. Wilhelm, T. Sivarani, B. Marsteller, J. A. Munn, C. A. L. Bailer-Jones, P. R. Fiorentin, and D. G. York, *Nature* **450**, 1020–1025 (2007), `0706.3005`.
111. R. Schönrich, M. Asplund, and L. Casagrande, *MNRAS* **415**, 3807–3823 (2011), `1012.0842`.
112. T. C. Beers, D. Carollo, Ž. Ivezić, D. An, M. Chiba, J. E. Norris, K. C. Freeman, Y. S. Lee, J. A. Munn, P. Re Fiorentin, T. Sivarani, R. Wilhelm, B. Yanny, and D. G. York, *ApJ* **746**, 34 (2012), `1104.2513`.
113. R. Schönrich, M. Asplund, and L. Casagrande, *ApJ* **786**, 7 (2014), `1403.0937`.
114. A. Frebel, E. N. Kirby, and J. D. Simon, *Nature* **464**, 72–75 (2010), `0912.4734`.
115. W. Aoki, P. S. Barklem, T. C. Beers, N. Christlieb, S. Inoue, A. E. García Pérez, J. E. Norris, and D. Carollo, *ApJ* **698**, 1803–1812 (2009), `0904.1448`.
116. J. Meléndez, L. Casagrande, I. Ramírez, M. Asplund, and W. J. Schuster, *A&A* **515**, L3 (2010), `1005.2944`.
117. S. G. Ryan, J. E. Norris, and T. C. Beers, *ApJ* **523**, 654–677 (1999), `astro-ph/9903059`.
118. S. G. Ryan, T. C. Beers, T. Kajino, and K. Rosolankova, *ApJ* **547**, 231–239 (2001), `astro-ph/0010413`.
119. K. Lind, F. Primas, C. Charbonnel, F. Grundahl, and M. Asplund, *A&A* **503**, 545–557 (2009), `0906.2876`.
120. O. Richard, G. Michaud, and J. Richer, *ApJ* **619**, 538–548 (2005), `astro-ph/0409672`.
121. A. J. Korn, F. Grundahl, O. Richard, P. S. Barklem, L. Mashonkina, R. Collet, N. Piskunov, and B. Gustafsson, *Nature* **442**, 657–659 (2006), `astro-ph/0608201`.
122. M. H. Pinsonneault, G. Steigman, T. P. Walker, and V. K. Narayanan, *ApJ* **574**, 398–411 (2002), `astro-ph/0105439`.
123. V. V. Smith, D. L. Lambert, and P. E. Nissen, *ApJ* **408**, 262–276 (1993).
124. V. V. Smith, D. L. Lambert, and P. E. Nissen, *ApJ* **506**, 405–423 (1998).
125. M. Asplund, and J. Meléndez, "Primordial and Pre-Galactic Origins of the Lithium Isotopes," in *First Stars III*, edited by B. W. O'Shea, and A. Heger, 2008, vol. 990 of *American Institute of Physics Conference Series*, pp. 342–346.
126. R. Cayrel, M. Steffen, H. Chand, P. Bonifacio, M. Spite, F. Spite, P. Petitjean, H.-G. Ludwig, and E. Caffau, *A&A* **473**, L37–L40 (2007), `0708.3819`.
127. T. C. Beers, G. W. Preston, and S. A. Shectman, *AJ* **103**, 1987–2034 (1992).
128. N. Christlieb, T. Schörck, A. Frebel, T. C. Beers, L. Wisotzki, and D. Reimers, *A&A* **484**, 721–732 (2008), `0804.1520`.
129. W. Aoki, T. C. Beers, Y. S. Lee, S. Honda, H. Ito, M. Takada-Hidai, A. Frebel, T. Suda, M. Y. Fujimoto, D. Carollo, and T. Sivarani, *AJ* **145**, 13 (2013), `1210.1946`.
130. S. C. Keller, B. P. Schmidt, M. S. Bessell, P. G. Conroy, P. Francis, A. Granlund, E. Kowald, A. P. Oates, T. Martin-Jones, T. Preston, P. Tisserand, A. Vaccarella, and M. F. Waterson, *PASA* **24**, 1–12 (2007), `astro-ph/0702511`.
131. R. Cayrel, E. Depagne, M. Spite, V. Hill, F. Spite, P. François, B. Plez, T. Beers, F. Primas, J. Andersen, B. Barbuy, P. Bonifacio, P. Molaro, and B. Nordström, *A&A* **416**, 1117–1138 (2004), `astro-ph/0311082`.
132. D. Yong, J. E. Norris, M. S. Bessell, N. Christlieb, M. Asplund, T. C. Beers, P. S. Barklem, A. Frebel, and S. G. Ryan, *ApJ* **762**, 26 (2013), `1208.3003`.
133. A. Helmi, M. J. Irwin, E. Tolstoy, G. Battaglia, V. Hill, P. Jablonka, K. Venn, M. Shetrone, B. Letarte, N. Arimoto, T. Abel, P. Francois, A. Kaufer, F. Primas, K. Sadakane, and T. Szeifert, *ApJ* **651**, L121–L124 (2006), `astro-ph/0611420`.
134. S. D. M. White, and V. Springel, "Where Are the First Stars Now?," in *The First Stars*, edited by A. Weiss, T. G. Abel, and V. Hill, 2000, p. 327, `astro-ph/9911378`.
135. J. Tumlinson, *ApJ* **708**, 1398–1418 (2010), `0911.1786`.
136. S. Salvadori, A. Ferrara, R. Schneider, E. Scannapieco, and D. Kawata, *MNRAS* **401**, L5–L9 (2010), `0908.4279`.
137. M. Ness, K. Freeman, E. Athanassoula, E. Wylie-de-Boer, J. Bland-Hawthorn, M. Asplund, G. F. Lewis, D. Yong, R. R. Lane, and L. L. Kiss, *MNRAS* **430**, 836–857 (2013), `1212.1540`.
138. T. Bensby, M. Asplund, J. A. Johnson, S. Feltzing, J. Meléndez, S. Dong, A. Gould, C. Han, D. Adén, S. Lucatello, and A. Gal-Yam, *A&A* **521**, L57 (2010), `1009.5792`.
139. G. Gilmore, S. Randich, M. Asplund, J. Binney, P. Bonifacio, J. Drew, S. Feltzing, A. Ferguson, R. Jeffries, G. Micela, I. Negueruela, T. Prusti, H.-W. Rix, A. Vallenari, E. Alfaro, C. Allende-Prieto, C. Babusiaux, T. Bensby, R. Blomme, A. Bragaglia, E. Flaccomio, P. François, M. Irwin, S. Koposov, A. Korn, A. Lanzafame, E. Pancino, E. Paunzen, A. Recio-Blanco, G. Sacco, R. Smiljanic, S. Van Eck, and N. Walton, *The Messenger* **147**, 25–31 (2012).
140. T. H. Greif, V. Springel, S. D. M. White, S. C. O. Glover, P. C. Clark, R. J. Smith, R. S. Klessen, and V. Bromm, *ApJ* **737**, 75 (2011), `1101.5491`.
141. S. Hirano, T. Hosokawa, N. Yoshida, H. Umeda, K. Omukai, G. Chiaki, and H. W. Yorke, *ApJ* **781**, 60 (2014), `1308.4456`.

APPENDIX: UNSOLICITED ADVICE FOR NEW PHD STUDENTS

Throughout my lecture series at the XVIII Ciclo de Cursos Especiais Advanced School at the Observatório Nacional in Rio de Janeiro in October 2013, I provided some unsolicited advice for new PhD students and students considering embarking on a career in astronomy. As they seem to have been well received and appreciated by the audience I include them here with some additional comments for completeness:

- **Choose your PhD project wisely:** It is very important to carefully consider the topic you are going to do your PhD thesis on as it will likely guide your whole future research career; most scientists will not stray too far away from their PhD topic and/or techniques learnt during it later in life. Do not choose your project by default for example by simply carrying on with your previous undergraduate supervisor. Look around at different options, not just in your home institutes, but also elsewhere, including abroad. Select a topic that you are passionate about – you will end up working very hard on your project during your PhD and that can only be enjoyable it you feel strongly about it personally. Preferably select a PhD topic in a research area that is starting to become very attractive or important, perhaps due to the advent of some new ground-breaking telescope and/or instrumentation, yet is not already over-crowded with other people. Try to find your own niche. Finally, discuss your thesis topic ideas with senior and junior colleagues to get their opinion before making up your mind but remember to still follow your own conviction.

- **Choose your PhD supervisor wisely:** As important as choosing your PhD project is to identify your supervisor. Do you want the "Big Deal", the "Young Spark" or the "Experienced" (a.k.a. old) supervisor? Each type has its own advantages and disadvantages and there are no general rule of thumb which is the best match for each student. Talk to your potential supervisor's past and current students to better understand his/her style of supervision to make sure it matches with your own expectations and preferences (e.g. what level of supervision can they provide). And most importantly, talk to many different potential supervisors about their research areas as well as their style of supervision – you will most likely discover that most areas of research are exciting when talking to somebody who is passionate about it and thus you may well end up choosing a topic you hadn't at all considered initially. Do not be afraid of contacting senior scientists asking them to supervise your PhD – all of us are only flattered by being considered as a possible supervisor!

- **Write, write, write:** This sounds better than the canonical *Publish or perish* but has a broader meaning. The most important medium scientists present the results of their hard work in is obviously scientific articles in refereed journals. In fact, when judging your abilities for any future job, prize etc, that is by far the most important criteria. You must learn to write scientific articles, which do have very distinct style, quite different from any other type of writing. Take courses early on how to write and structure papers. Articles do not need to be literature masterpieces but must convey the motivation, methodology, main results and interpretations in a logical and straightforward manner. Do not ever let writer's block overcome you! Ensure that you write something, anything really, every day, for example a small report to your supervisor describing what you have achieved with questions how to continue or just keep your own journal log of your work. By continuously writing about your work, it will make it vastly simpler when you want to turn your results into a published paper.

- **Automate everything:** You might as well accept it early on: you will redo and redo and redo everything during your PhD so it is much better to automate everything the first time or at least the second time. Don't waste your time with repetitive time-consuming medial tasks. Automating things will also ensure repeatability, which is vital in science. Consider how every task you do can be streamlined and made more efficient.

- **Learn project and time management:** Doing a PhD is a major undertaking and should be approached as such. Whatever the nominal allocated time for your PhD in your home institution is, chances are that most, if not all, students end up with a great rush and panic at the end to finish everything in time. Structure your project into sub-projects with clear goals and deadlines and stick to them. Learn how *you* work most efficiently (e.g. are you a morning/afternoon/evening person for writing, meetings, researching etc?). Don't waste your time unnecessarily by being distracted: set aside some time in your schedule for goofing around/surfing the net/talking to your fellow students etc if you feel you need it but then promise yourself that for the rest of the time you will work effectively on your research project and keep to it. Schedule long, completely uninterrupted (switch off phone, email, twitter, whatever!) periods each day for serious thinking/researching/writing that requires full concentration and do not let other people interfere with that time in any way. Most likely your university will hold workshops on project and time management techniques for students and early career researchers – attend them early on!

- ***"Never underestimate your audience willingness to hear something they already know":*** This is arguably the best advice I ever received from my former PhD supervisor (among many other great snippets of wisdom he passed on to me and his other students and colleagues). Learn how to give a *great* talk and don't be satisfied until you know how to capture your audience' attention for the entire allocated time, be it 1min, 10min, 30min or 1hr. The vast majority of talks at scientific conferences and institutions are frankly rather uninspiring, mainly because the talk does not have sufficient background and motivation to the project and too quickly veer into unnecessary detail and technicalities that are not important for more than a very small minority of the audience, if at all. Oral presentations have a remarkably small bandwidth for transferring information so keep repeating the main take home message you want to convey and help the listener by repeatedly going back to the main story you are telling in case they loose the thread somewhere along the line. Giving excellent talks is a skill that everybody can acquire and should do. Again, there are plenty of courses both online and at your university how to give oral presentations so there is no excuse not to learn it. Give presentations at every opportunity and attend other talks with a view to figure out what presentation techniques/styles work (and what does not!).

- **Know your target audience:** Part of giving a good talk is to know who you are speaking to and their likely background and level of knowledge and adjust your presentation accordingly. Remember that you need to get to their level, not the other way around. This is true also in other situations such as writing observing or grant applications. Find out beforehand who will review the application: are they experts in your field, general astronomers or perhaps not astronomers at all? Your application should obviously look very differently with far less detail for the latter cases (e.g. can you really expect the reader/listener to know that acronym you are using?). Try putting yourself in their situation, reminding yourself that reviewers of observing and grant proposals most of the time are under extreme time pressure; they may have at most 30min in total to spend on your application, from reading it to formulating their opinion and feedback, so make it easier for them: use executive summaries, highlight the most important take-home message(s) (but do not go overboard with boldface!), remove unnecessary clutter and detail and keep the story you are trying to convey simple and straight (the KISS principle: "Keep it simple, stupid").

- **Ensure that senior scientists know your work:** Whether you like it or not, fact of the matter is that your career will be judged by more senior scientists. They will likely determine whether you will have a chance to continue in academia so you'd better ensure that they know about you and have a positive opinion of your work. Seek them out at conferences to discuss your work and/or send them an email updating them of your progress, perhaps asking them for advice how to interpret your latest results. Ask to come and visit their institution and research groups to establish new collaborations. Always volunteer to give a talk at conferences (to be honest, nobody really cares about posters but people will remember who you are when you have stood up in front of everybody and delivered a great talk – see above).

- **Keep a healthy work-life balance:** No need to explain this really – this is true whatever you choose to do work-wise. Make sure you have something else to clear your head with whatever that may be when things are not going so well with your research project (which undoubtedly will happen occasionally). Everybody needs to regularly switch off and regenerate the batteries.

- **Enjoy it!** You are about to embark on the best possible career I can imagine so embrace it fully and completely. You will have an opportunity to get paid to do your hobby, hang out and learn from some amazingly clever, inspiring and like-minded people, visit some of the coolest places on Earth and play with some truly expensive toys while all of your family, friends and new people you will meet will think it is amazing and fascinating that you are (studying to become) an astronomer. If you don't enjoy doing this you have made the wrong choice and there is nothing wrong with that, just go and do something else instead. If you do love it on the other hand, I can only congratulate you and welcome you to the club!